Ali, Linda Zaidoon

STUDIES OF THE KINETIC MECHANISM AND THE SUBUNIT STRUCTURE OF HYPOXANTHINE-GUANINE PHOSPHORIBOSYL TRANSFERASE FROM SACCHAROMYCES CEREVISIAE

City University of New York PH.D. 1982

PLEASE NOTE:

In all cases this material has been filmed in the best possible way from the available copy. Problems encountered with this document have been identified here with a check mark ✓.

1. Glossy photographs or pages ✓
2. Colored illustrations, paper or print _____
3. Photographs with dark background ✓
4. Illustrations are poor copy _____
5. Pages with black marks, not original copy _____
6. Print shows through as there is text on both sides of page _____
7. Indistinct, broken or small print on several pages ✓
8. Print exceeds margin requirements _____
9. Tightly bound copy with print lost in spine _____
10. Computer printout pages with indistinct print _____
11. Page(s) _____ lacking when material received, and not available from school or author.
12. Page(s) _____ seem to be missing in numbering only as text follows.
13. Two pages numbered _____. Text follows.
14. Curling and wrinkled pages _____
15. Other _____

Studies of the Kinetic Mechanism and the Subunit Structure of Hypoxanthine-Guanine Phosphoribosyltransferase From *Saccharomyces cerevisiae*

by

Linda Z. Ali

A dissertation submitted to the Graduate Faculty in Biochemistry in partial fulfillment of the requirements for the degree of Doctor of Philosophy, The City University of New York.

1981

This manuscript has been read and accepted for the Graduate Faculty in Biochemistry in satisfaction of the dissertation requirement for the degree of Doctor of Philosophy.

10/23/81
Date

Chairman of Examining Committee

December 18, 1981
Date

Executive Officer

Supervisory Committee

ABSTRACT

Studies of the Kinetic Mechanism
and the Subunit Structure of
Hypoxanthine-Guanine Phosphoribosyl-
transferase from Saccharomyces
cerevisiae

by

Linda Z. Ali

Adviser: Professor Donald L. Sloan

Hypoxanthine-guanine phosphoribosyltransferase (HG-PRTase) has been purified to homogeneity from baker's yeast extracts using GMP-Sepharose chromatography and has been utilized to determine the molecular weight and the subunit structure of the enzyme. The native molecular weight determined by Sephadex G-100 column chromatography was 52,000. After treatment with sodium dodecylsulfate, a single band with an apparent molecular

weight of 26,000 was observed using sodium dodecylsulfate polyacrylamide gel electrophoresis. Chemical cross-linking with glutaraldehyde and dimethylsuberimidate with subsequent SDS-polyacrylamide gel electrophoresis resulted in two protein species with molecular weights of 26,000 and 52,000. These results suggest that the enzyme consists of two very similar, probably identical subunits.

The purified enzyme was also utilized to characterize the simultaneous formations of inosine monophosphate (IMP) and guanosine monophosphate (GMP) in solutions containing hypoxanthine, guanine and 5-phosphoribosyl α-1-pyrophosphate. The time-dependent changes in concentrations of the substrates and products were monitored using a Brownlee MPLC ion-exchange column and high pressure liquid chromatography (HPLC). Elution times for hypoxanthine, guanine, IMP and GMP through this column were 1.3, 1.7, 2.3 and 3.8 min. respectively. This procedure allowed two calculations of three initial velocities (PRibPP utilization, IMP formation and GMP formation) from a single set of results where the H-to-G concentration ratio was varied over a range of solution PRibPP concentrations. Double-reciprocal plots of these rates vs substrate concentrations, fashioned after the "one product" and "common product" theories for alternate-substrate kinetic analysis of Huang (Meth. Enzymol. 63, 486,

1979), revealed that these enzymatic reactions proceed through the use of an Ordered BiBi kinetic mechanism with guanine characterized as the highly preferred substrate.

This proposed kinetic mechanism was confimred by flow dialysis and isotope exchange experiments. The formation of binary purine-base complexes with HG-PRTase were not detected whereas a PRibPP-enzyme interaction was observed. Moreover only minimal exchange between GMP and C^{14}-guanine, and between IMP and C^{14}-hypoxanthine were observed when these substrate/product pairs were incubated with the enzyme. Thus random and ping pong kinetic mechanisms each appear to be unlikely as the sequence through which yeast HG-PRTase proceeds. However, substantial exchange of label did occur when PRibPP and P^{32}-PP_i were incubated with HG-PRTase suggesting that cleavage of the pyrophosphate group may not depend upon the presence of guanine or hypoxanthine but may be accelerated by base addition. The kinetic data were then analyzed using equations which describe an Ordered BiBi kinetic mechanism and the K_m values for hypoxanthine (26±2 um) guanine (41±3 uM) and PRibPP (49±5 uM) were calculated. The V_{max} values for IMP formation (170±14 units/mg) and GMP formation (640±70 units/mg) verify the preference for guanine as substrate for this enzyme.

TABLE OF CONTENTS

LIST OF TABLES

LIST OF FIGURES

LIST OF FIGURES (cont'd)

INTRODUCTION

Purine Phosphoribosyltransferases. Two purine salvage enzymes in man catalyze the transfer of the ribose-5-phosphate moiety of 5-phosphoribosyl ∝-1-pyrophosphate (PRibPP)[1] to purine bases to form the corresponding nucleotides. The highest levels of these enzymes are found in cells that have a limited capacity for de-novo purine biosynthesis, such as erythrocytes, leukocytes and nerve cells.

Adenine phosphoribosyltrasferase (E.C.2.4.2.7) catalyzes the conversion of adenine to adenosine-5'-monophosphate (equation 1). A related enzyme, hypoxanthine-guanine phosphoribosyltransferase (E.C.2.4.2.8, HG-PRTase) catalyzes the formation of inosine-5'-monophosphate (IMP) from hypoxanthine and phosphoribosyl ∝-1-pyrophosphate (PRibPP) or the formation of guanosine-5'-monophosphate (GMP) from guanine and PRibPP (equations 2 and 3).

---

[1]Abbreviations. PRibPP, 5-phosphoribosyl ∝-1-pyrophosphate; HG-PRTase, hypoxanthine-guanine phosphoribosyltransferase; IMP, inosine-5'-monophosphate; GMP, guanosine-5'-monophosphate; AMP, adenosine-5'-monophosphate.

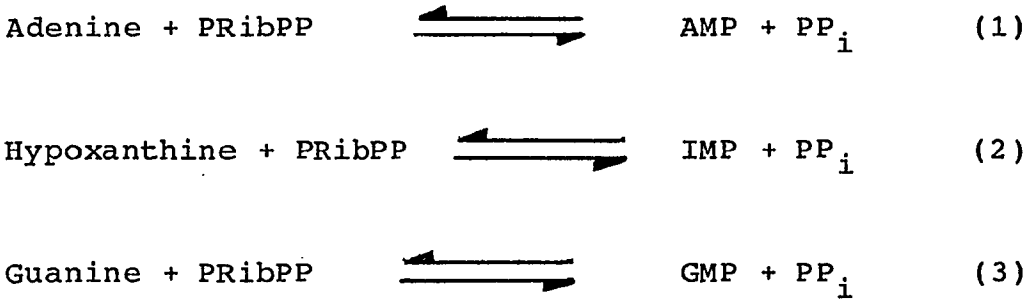

The enzyme, HG-PRTase also catalyzes the conversion of xanthine to xanthosine-5'-monophosphate (1). In addition, the purine analogs, 6-mercaptopurine, 6-thioguanine and 8-azaguanine also serve as substrates for HG-PRTase. In general terms, the enzyme binds effectively to purine bases which have either an oxo- or thio-group in position 6 and not to those with an amino group in this position (1). Binding is enhanced by an amino group at position 2 and diminished by a hydroxy group at this position. PRibPP is the only compound known to serve as the phosphoribosyl donor in these reactions (1).

This enzyme has been isolated from several mammalian tissues (2-5), bacteria (6), protozoa (7), human erythrocytes (8,9), and from two strains of yeast (10,11). Currently, attention is being given to studies of the states of subunit association of HG-PRTase from several sources, and evidence has been obtained suggesting that the enzymes from brain (2,12) and liver (3) exist as

trimers under specific conditions (13). In contrast HG-PRTase from human erythrocytes may exist predominantly as a tetramer (9,14) whereas it has been reported that yeast HG-PRTase is a monomeric species (11) with a molecular weight equivalent to two subunits of the mammalian enzymes.

Kinetic analyses of most of the above-described enzyme preparations have been initiated. A wide range of base and PRibPP K_m values have been reported (2-11). The lowest K_m values (0.42 uM for guanine and 2.9 uM for PRibPP) have been calculated from kinetic studies of the beef brain HG-PRTase (5) whereas the highest K_m values (120 uM for hypoxanthine, 200 uM for PRibPP) were obtained with a bacterial enzyme (6). A great deal of kinetic information has been collected concerning HG-PRTase from human erythrocytes which has been shown to catalyze the synthesis of IMP through the use of an Ordered BiBi kinetic mechanism (8) although the release of products from the enzyme appears to be a random dissociation (8). Earlier studies had suggested that this HG-PRTase may utilize a ping-pong kinetic mechanism under specific conditions (15-17).

Phosphoribosyl α-1-pyrophosphate Metabolism. Intracellular metabolism is a highly coordinated system that is regulated by a wide variety of interrelated control mechanisms.

Metabolism presents many interesting questions and problems which account for the wide interest shown by workers representing many disciplines. For example, the organic chemist is interested in questions concerning the chemistry of intermediates in the reaction and the mechanisms of these transformations. The biochemist is concerned with metabolism and its control from the point of view of the relationship between the simplified systems studied in-vitro and events in the living cell (in-vivo), whereas the alterations in metabolism brought on by diseased states are of primary concern to the physician or medical scientist. Therefore the ultimate goal of the study of metabolism is a complete understanding of all reactions of living cells from all points of view, including their interactions with and interdependence upon control systems in normal and diseased states.

In the regulation of a metabolic pathway, the concentration of the enzymes as well as the specific substrates, activators and inhibitors of the enzyme are important. There are some compounds that serve as a substrate for more than one metabolic pathway. In order for these compounds to be apportioned through these various metabolic pathways, it is necessary that its intracellular

concentration be closely regulated. The high energy sugar phosphate, (PRibPP) initially discovered by Kornberg (18), is an essential substrate for several different metabolic pathways in the synthesis of purines, pyrimidines and pyridine nucleotides and is probably necessary for the survival and growth of all cells. PRibPP was shown to play a critical role in the regulation of purine synthesis de-novo in man (19). One line of evidence supporting the role of PRibPP in this regulation process came from studies of cultured human fibroblasts and erythrocytes of patients with inherited abnormalities of human PRibPP synthetase, in which the structural mutant form of the enzyme leads to increased PRibPP synthesis in conjunction with purine nucleotide overproduction and clinical gout (20, 21). The structural gene for this enzyme has been mapped on the X-chromosome (22).

The synthesis and degradation of PRibPP occur by many different pathways. The enzyme PRibPP synthetase (E.C.2.7.6.1) catalyzes the synthesis of PRibPP from ATP and ribose-5-phosphate in a reaction that requires magnesium and inorganic phosphate (equation 4).

$$\text{Ribose-5-phosphate} + \text{ATP} \rightleftharpoons \text{PRibPP} + \text{AMP} \qquad (4)$$

PRibPP Synthesis. Studies of the synthesis of PRibPP in Escherichia coli (23), Ehrlich ascites tumor cells (24) and human tissues (25) suggest that the regulaton of PRibPP synthesis is quite complex and is dependent upon the availability of ribose-5-phosphate, the energy level of the cell and feedback inhibition from end products. In mammalian cells the rate of PRibPP synthesis is dependent on the availability of ribose-5-phosphate. Glycolytic intermediates play an important role in the regulation of ribose-5-phosphate concentration in Ehrlich ascites tumor cells. As a result, PRibPP synthesis is stimulated by glucose, fructose and mannose, whereas iodoacetate and dinitrophenol inhibit its synthesis (24). Increasing the level of ribose-5-phosphate via the hexose-monophosphate shunt also increases the synthesis of PRibPP in red blood cells (26). Moreover, analysis of the kinetic mechanism of the purified PRibPP synthetase from Salmonella typhimurium (27) and rat liver (28,29) demonstrated that the enzyme activity is influenced by a number of effector compounds including substrates, inhibitors, activators and products. In addition, the enzyme displayed Michaelis-Menten kinetics. The K_m values for the substrate, ribose-5-phosphate were 3.3×10^{-5}M and 1.6×10^{-4}M for the enzyme purified from human erythrocytes (30) and Salmonella typhimurium (31) respectively.

The kinetic mechanism of the enzyme from Salmonella typhimurium was defined as an Ordered BiBi mechanism with magnesium-ATP binding first and PRibPP was released last (31). The enzyme from human erythrocytes also exhibited an Ordered BiBi mechanism, but product inhibition studies suggested that ribose-5-phosphate was bound first and PRibPP was released last (30). These studies also demonstrated that a hydroxyl group at position 2 and a phosphate at position 5 of the ribose moiety were required for binding to the enzyme. The values of the Michaelis constant for the second substrate, Mg^{2+}-ATP, were $1.4x10^{-5}$M and $4.6x10^{-5}$M for the purified enzyme from human erythrocytes (30) and Salmonella typhimurium (31) respectively. Removal of inorganic phosphate resulted in a complete loss of enzyme activity (30). A divalent cation, such as Mg^{2+} or Mn^{2+} is also required for enzyme activity, with magnesium being the most effective for enzymatic activity (30).

Studies of the enzyme from different sources suggest that inhibitors interact with the PRibPP synthetase at one of three different sites. The inhibition by ADP is competitive with respect to Mg^{2+}-ATP (23,30, 31), the K_i for ADP is $1.0x10^{-2}$mM which is below its intracellular concentration in most mammalian tissues (30). The enzyme is also inhibited in-vitro by 2,3-diphosphoglycerate and

PRibPP, both of which compete with ribose-5-phosphate (26,30). PRibPP does not seem to be an important inhibitor of its own synthesis, since the observed K_i value of $5x10^{-2}$mM is about ten times greater than its intracellular concentration in human erythrocytes (19). In contrast to PRibPP, 2,3-diphosphoglycerate seemed to be an important factor in the control of PRibPP synthesis in this tissue (30), since its K_i value was found to be approximately equal to its intracellular level (5.3 mM). In addition to inhibition by ADP and 2,3-diphosphoglycerate, a large number of compounds including AMP, GDP, GTP, IDP, ITP, NAD, NADH and FAD also inhibit PRibPP synthetase by a non-competitive mechanism. The diphosphate and triphosphate deriveratives were shown to have a more potent inhibitory effect than the monophosphates (30). In contrast to the enzyme from human cells the enzyme from S. typhimurium was shown to be inhibited specifically by uridine nucleotides and not by any other purine or pyrimidine ribonucleotides (32).

PRibPP synthetase isolated from human erythrocytes was shown to undergo a reversible association and dissociation under appropriate conditions. The native molecular weight of the human erythrocyte enzyme was 60,000 in the absence of substrates. Sodium dodecylsulfate gel

electrophoresis gave a subunit molecular weight of 34,500. However, in the presence of a saturating concentration of magnesium chloride and ATP, the enzyme associated into two heavy forms with molecular weights of 72,000 and 1,200,000 (25). Inhibition by ADP had no effect on the molecular aggregation of the enzyme. Based on these results these investigators concluded that the aggregated form is the active form of the enzyme and that the enzyme normally existed in an aggregated form in the cell, since the concentrations of magnesium and ATP required to induce aggregation were within the normal intracellular level found in the human erythrocytes.

PRibPP Degradation. The degradation of PRibPP occurs by a class of enzymes known as the phosphoribosyltransferases which are widely distributed in nature. Examples of this degradation are provided in equations 1-3. These enzymes catalyze the transfer of the ribose-5-phosphate moiety of PRibPP to a nitrogenous base. In the de-novo synthesis of purine nucleotide the nitrogenous base is either the amide of glutamine or ammonia (33), whereas free bases serve as nitrogen donors during the synthesis of pyrimidine nucleotides (34) and purine nucleotides using the previously described salvage pathways (35). In addition, nicotinic acid serves as the nitrogen donor for NAD

synthesis (36), anthranilate serves as the nitrogenous base for tryptophan synthesis (37) and ATP is the nitrogen donor for histidine synthesis (38). All these reactions can be written in general as shown in equation 5.

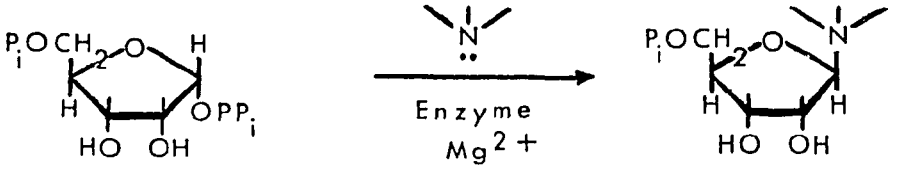

(5)

In the study of inherited abnormalities of man, the demonstration of variations in the properties of these enzymes have provided evidence for mutations of the structural genes coding for these proteins. Different variants from the normal have suggested the heterogeneous nature of these mutations (39). A wealth of evidence now favors the view that serum uric acid levels are the result of an intricate interaction of many factors. Although hyperuricemia is frequently acquired in nature, it can also be caused by an inborm error of metabolism in man. In order to understand the biochemical basis of this increased production of uric acid, extensive studies of the enzymes involved in purine biosynthesis have been

undertaken. Direct evidence was provided for alterations of the enzymes, PRibPP synthetase, PRibPP amidotransferase and HG-PRTase in patients with gout.

A structurally abnormal form of the enzyme PRibPP synthetase was isolated from the cultured fibroblasts of a young male patient with increased uric acid production (21). The mutant enzyme possessed superactive catalytic properties and was resistant to feedback inhibition by purine nucleotides (ADP and GDP). The enzyme, PRibPP amidotransferase (E.C.2.4.2.14) catalyzes the transfer of the amide nitrogen of glutamine to the phosphoribosyl moiety of PRibPP to form 5-phosphoribosyl-1-amine, inorganic pyrophosphate and glutamate and is the first committed step of de-novo purine biosynthesis (Figure 1). An increase in this enzymatic activity was observed in cultured fibroblasts from patients with the Lesch-Nyhan syndrome. This increase was due apparently to an increase in the intracellular concentration of PRibPP rather than from an intrinsic increase in the amount of enzyme. A deficiency of HG-PRTase is also associated with uric acid overproduction and hyperuricemia (40). HG-PRTase deficiency as well as PRibPP synthetase hyperactivity enhance the availability of PRibPP which seems to stimulate purine biosynthesis de-novo (41).

Figure 1. A) Glutamine phosphoribosylpyrophosphate amidotransferase catalyzes the first reaction of purine biosynthesis de novo. B) The catabolism of purine nucleotides proceeds through 1) 5'-nucleotidase, 2) adenosine deaminase, 3) adenosine kinase, 4) purine nucleoside phosphorylase and 5) xanthine oxidase. C) The salvage of the purine bases to form their respective nucleotides proceeds through 6) hypoxantine-guanine phosphoribosyltransferase and 7) adenine phosphoribosyltransferase.

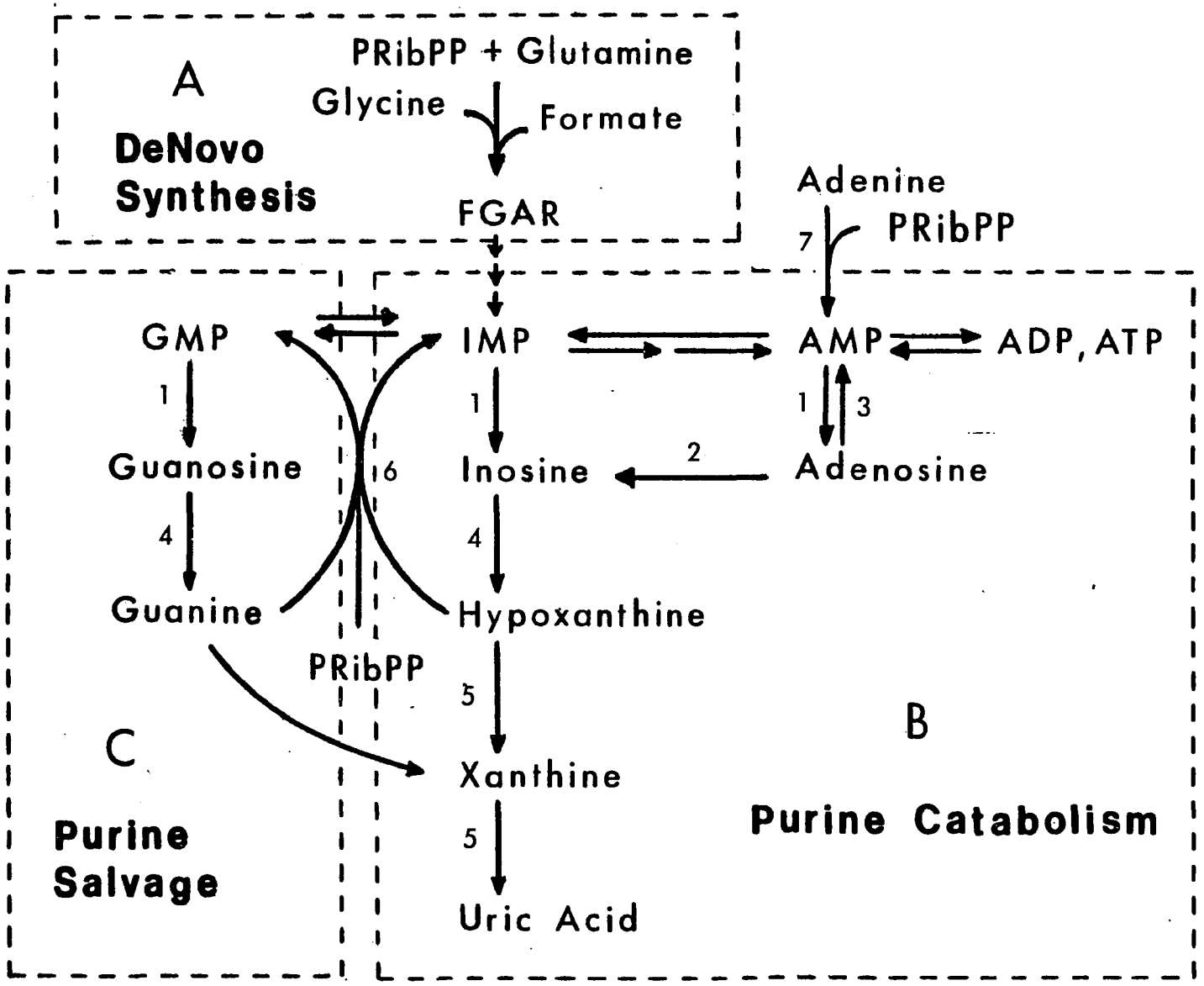

Figure 1. Purine metabolism.

Effects of Purine Metabolism on Other Metabolic Pathways. Erythrocytes from individuals with HG-PRTase deficiencies show an increase of several other enzyme activities which are not directly associated with purine metabolism. The activities of four enzymes, aspartate transcarbamylase, dihydroorotase, orotate phosphoribosyltransferase and orotidylate decarboxylase, required for the biosynthesis of pyrimidines de-novo, were increased two to ten fold in erythrocytes of individuals with HG-PRTase deficiency (42,43). The mechanism responsible for the increased activities of these enzymes has not been established. Interestingly, increases in the activities of the enzymes associated with pyrimidine biosynthesis was limited to erythrocytes and these effects were not observed in leukocytes or fibroblasts.

Recent studies also demonstrated a partial deficiency in the enzyme, S-adenosylhomocysteine hydrolase in the erythrocytes of patients with genetic deficiencies of purine nucleoside phosphorylase and HG-PRTase (44). The enzymes, adenosine deaminase, purine nucleoside phosphorylase and HG-PRTase catalyze sequential steps in the interconversion of purine nucleosides and reutilization of purine bases (Figure 1). Moreover, adenosine deaminase deficiency leads to a severe combined

immunodeficiency with T-cell and B-cell dysfunction. Purine nucleoside phosphorylase deficiency results in an immunodeficiency disease with a specific defect in T-cell function as well as de-novo overproduction of purine. S-adenosylhomocysteine hydrolase catalyzes the reversible cleavage of S-adenosylhomocysteine to adenosine and L-homocysteine. In the absence of S-adenosylhomocysteine hydrolase, there is an accumulation of S-adenosylhomocysteine which is both a product and inhibitor of S-adenosylmethionine-dependent transmethylation reactions. A deficiency of this enzyme in HG-PRTase deficient individuals was investigated in order to evaluate its possible role in producing the immunologic or neurologic abnormalities in these individuals. Hypoxanthine did not inactivate purified S-adenosylhomocysteine hydrolase but inosine caused a phosphate-dependent irreversible inactivation of the purified enzyme and of the enzyme in intact erythrocytes and cultured lymphoblastoid cells deficient in HG-PRTase (44). In order to explain these results, these investigators suggested that in HG-PRTase deficient cells, hypoxanthine was able to shift the equilibrium of the nucleoside phosphorylase reaction to inosine thus preventing the breakdown of inosine. This would account for the partial deficiency of S-adenosylhomocysteine hydrolase in HG-PRTase deficient patients.

The Lesch-Nyhan Syndrome. HG-PRTase was originally referred to as a salvage enzyme of purine metabolism since it provides a mechanism for the reutilization of free purine bases that would be otherwise oxidized and excreted as uric acid. The importance of this enzyme was first recognized by Seegmiller et al (40) who found that a complete deficiency of this enzyme in man was the basis for the excessive production of uric acid found in patients with the Lesch-Nyhan syndrome, an inherited X-linked disorder characterized by self-mutilative behavior, choreoathetoid cerebal palsy, hyperuricemia, as well as growth and severe mental retardation (45). Subsequently identified was a less severe defect of the same enzyme in patients with gout due to an excessive production of uric acid and no detectable neurological abnormality (46).

The Lesch-Nyhan syndrome occurs exclusively in males (47). A mutation in a structural gene on the X-chromosome is responsible for this disease (vide-infra). Patients suffering from this syndrome appear normal at birth even though the primary enzyme defect accompanied by uric acid overproduction are present. These children continue to develop normally for the first six to eight months. Then infants, who have been holding their heads up and have been sitting, begin to lose these abilities. In the

established disease, the motor defect is of greater severity than the defect in intelligence. The most striking feature of this syndrome is an aggressive, self-destructive behavior. Self-mutilation takes the form of biting away the lips, tongue and ends of the fingers in a compulsive manner. These patients are sensitive to pain and are happy to be securely protected from themselves. Extraction of the teeth had a beneficial effect in many cases. Certain patients are also known to direct their aggression against others and as they learn speech, they become verbally aggressive.

The Lesch-Nyhan syndrome is the first known instance in which a stereotyped pattern of abnormal human behavior is associated with a distinct metabolic abnormality. These individuals also develop a number of clinical symptoms that are directly related to the overproduction of uric acid. As a consequence, they develop acute arthritis, hematuria, crystalluria and urinary tract stones. The severe neurological disorder associated with a complete deficiency of HG-PRTase in the Lesch-Nyhan syndrome was the first piece of evidence to demonstrate the importance of HG-PRTase to the normal function of mammalian cells. Also, the excessive overproduction of uric acid found in individuals with a partial deficiency

of this enzyme provided the first indication of the importance of the "Salvage Pathway" of purine metabolism especially the role of HG-PRTase in regulation of the rate of purine biosynthesis.

The first evidence of metabolic abnormality is a high level of uric acid in the blood and an increase in the amount of uric acid excreted in the urine. This increase in uric acid production and overexcretion was attributed to an increase in de-novo purine synthesis. The mechanism for the overproduction of uric acid was investigated in-vivo by measuring the rate at which uric acid was synthesized from [^{14}C]-glycine (48). During de-novo synthesis, incorporation of glycine into the purine ring labels IMP which can then be degraded to inosine, hypoxanthine, xanthine and uric acid. Based on these observations, these investigators concluded that the increase in the rate of incorporation of [^{14}C]-glycine into urinary uric acid found in individuals with a deficiency of HG-PRTase resulted from an increase in the de-novo purine synthesis. They overlooked the fact that uric acid overproduction in HG-PRTase-deficient cells could result from the inability to resynthesize IMP from hypoxanthine. In the absence of HG-PRTase, hypoxanthine is oxidized to uric acid. Therefore, the observed increase

in uric acid production from the incorporation of [^{14}C]-glycine may be due to a decrease in the reutilization of hypoxanthine as well as an increase in de-novo synthesis. In order to determine the relative contribution of a disorder of hypoxanthine salvage to uric acid over-production in HG-PRTase-deficient cells, [8-^{14}C]-adenine or [8-^{14}C]-inosine was administered intravenously to nine patients with normal HG-PRTase activity, three with a partial deficiency of this enzyme and six with the classical Lesch-Nyhan syndrome (49). The results showed that a decrease in hypoxanthine reutilization was an important contributor to uric acid overproduction and confirmed that the purine salvage pathway was an important mechanism for the reutilization of hypoxanthine in man.

In addition to the complete syndrome, variants of the syndrome have been found that differ primarily in the degree of neurological abnormalities and the level of uric acid overproduction. Currently, a wealth of information has accumulated favoring the view that a HG-PRTase deficiency results from different types of mutations in the structural gene. Genetic heterogeneity of HG-PRTase deficiency was demonstrated also by variations in the enzyme kinetic and physical properties. Mutant enzymes with altered substrate affinities (50), lowered

susceptibility to product inhibition (51), decreased heat stability (52) and altered electrophoretic mobilities (53) were revealed by enzymologic characterization. The hemolysates from four patients with a partial deficiency of HG-PRTase were evaluated by the isoelectric focusing technique (53). The isozymes of the HG-PRTase from normal human hemolysate have isoelectric pH values between 5.6 and 6.1 (53,54). In contrast the hemolysates of these four patients had isozymes with pH values between 5.3 and 5.9. These results suggest that the mutant enzymes had an altered electrical charge and this was not the consequence of a modified carbohydrate moiety since HG-PRTase is not a glycoprotein (55).

A complete lack of HG-PRTase is usually accompanied by the neurological features of the Lesch-Nyhan syndrome, while the less severe enzyme deficiency gives rise to gouty arthritis. The residual HG-PRTase activity in erythrocytes of individuals with the Lesch-Nyhan syndrome is usually less than 1% of the normal (56) while the residual activity in cultured skin fibroblasts derived from those patients varies from 0.6 to 7% (57). Residual activities in erythrocytes and fibroblasts from patients with a partial deficiency of HG-PRTase are usually much higher and range up to 30% of the normal, and these

patients have few or no neurological symptoms but have problems related only to the overproduction of uric acid (56). However, exceptions to this rule have been reported. A patient was described with the classical Lesch-Nyhan syndrome but having a residual HG-PRTase activity between 5 to 10% in erythrocytes and about 30% in fibroblast lysate (58), although the activities of the other enzymes of purine metabolism fitted the classical Lesch-Nyhan syndrome. For example, there was an increase in the activities of adenine phosphoribosyltransferase and adenosine deaminase, whereas the activities of adenosine kinase and PRibPP synthetase were normal. Due to the unusually high residual activity, the mutant enzyme was characterized enzymatically in erythrocytes and fibroblasts. In fibroblasts the affinity for the substrates, hypoxanthine and guanine, were normal (K_m for hypoxanthine ranged from 0.04-0.06M, K_m for guanine was 0.03mM) while there was an increase in the affinity for PRibPP (K_m PRibPP - 1.1mM). The K_m of the erythrocyte enzyme for hypoxanthine was also increased (K_m 0.063-0.097mM). There was a complete absence of product inhibition by IMP and GMP as well as a decreased heat stability. The addition of PRibPP did not stabilize the enzyme.

Immunoprecipitation experiments with an antibody raised against normal HG-PRTase showed the presence of an approximately normal amount of material cross-reacting with anti-human HG-PRTase antiserum (58). After repeated freezing-thawing of the sample, no cross-reacting material was detected. This illustrated that the mutant HG-PRTase molecule was unstable. From these studies (58) these investigators concluded that the primary defects of the mutant enzyme was a structural mutation affecting the PRibPP site of the enzyme. The erythrocytes of the patient's mother had a normal HG-PRTase activity with normal enzyme characteristics. However, her fibroblasts had a lower HG-PRTase activity, a decrease in the heat stability of the enzyme, but a normal affinity for PRibPP. Hair root analysis of several members of the patient's family confirmed that the mother was a heterozygous carrier.

Genetic Considerations. According to the Lyon hypothesis (59), one of the two X-chromosomes in the female mammalian cell is randomly inactivated at an early stage of embryonic development to form the Barr body. This inactivation is initially random in placental females such that in any given cell either the paternal- or the maternal-X can become the inactive X-chromosome. Once

established, the pattern of X inactivation seems to be permanent in somatic cells. As a consequence, all descendants of a particular early embryonic cell maintain the same inactive X-chromosome through many cell generations. Moreover, reexpression of an inactive X-gene was shown to occur at a low frequency in mouse-human cell hybrids (60).

The molecular nature of X-chromosome inactivation was examined by the techniques of DNA-mediated cell transformation of the X-linked HG-PRTase locus (61). These experiments were designed to determine whether purified DNA from HG-PRTase mutant female mouse cell line CAK, that carried a HG-PRTase mutation of the active X-chromosome and a presumed wild-type HG-PRTase allele on the inactive one, was capable of transformation for HG-PRTase. The results showed that purified DNA from the inactive X-chromosome of the CAK mouse cell line was not effective in transformation for HG-PRTase, but the DNA from the active X-chromosome was capable of transformation for HG-PRTase. These observations imply that the DNA of the inactive X-chromosome at or near the HG-PRTase locus differed in some fashion from the DNA of the corresponding active X-chromosome and this difference could account, at least in part, for its inactivation. These investigators

speculated that the difference could involve modification of either the active or inactive X-DNA, caused by methylation or some other DNA sequence changes.

DNA-mediated cell transformation technique was applied to transfer HG-PRTase via purified DNA from wild-type Chinese Hamster Ovary cells into cultured mouse cells deficient in HG-PRTase activity (62,63). This method of transformation is useful in detecting the presence of specific genes in a DNA preparation and can be employed as a bioassay to monitor the purification of a particular gene by a combination of biochemical and cloning techniques. The transformation technique is a useful bioassay since it does not depend on the abundance of the gene product, but, on the availability of an appropriate selective system. The X-linkage of this "hprt-gene" facilitated the isolation of the enzyme deficient mutant, since only one copy of each X-linked gene is functional in most mammalian cells. Transformation of the hprt-gene using purified DNA represents one approach to the cloning of this sequence. Willecke et al (62) have described the intraspecies DNA-mediated transfer of the mouse HG-PRTase gene into HG-PRTase deficient mouse A9 cells. DNA was purified from the abnormal HG-PRTase revertant mouse BW5147-V1 cells and incubated with mouse A9 cells (which are HG-PRTase

deficient mouse L-cells). After growth in selective media, one clone was isolated which expressed the electrophoretically abnormal form of HG-PRTase. Six clones showed the normal form of HG-PRTase due to reversion of the defective HG-PRTase locus in A9 cells. This result indicated a DNA-mediated transfer of the mouse HG-PRTase gene at a frequency of about $0.5x10^{-7}$. Although this present method of DNA-mediated gene transfer is of relatively low efficiency, it still allows for the detection of the biological activity of the HG-PRTase gene. This system can also be employed to study the uptake expression of genes located in chemically modified total cellular DNA and it can be used as an assay to study the functional expression during the purification of single copy genes.

Recent studies also show that the adenovirus type-2, as well as the chemical compounds ethyl methanesulfonate and nitrosoguanidine, induce mutations at the HG-PRTase locus of Chinese hamster cells and suggest that these mutations occur through similar mechanisms (64,65). RJK3 and RJK39 are clones of Chinese hamster cells, which Kruh et al (65) selected, that were 8-azaguanine resistant after treatment of the wild type cells with nitrosoguanidine and ethyl methanesulfonate respectively. The cell extracts of RJK39 had no detectable HG-PRTase activity but the cell

extracts of RJK3 had 25% of the wild type value. Purified HG-PRTase from the wild type, RJK3, RJK39 and RJK39 revertants, labeled in-vivo with radioactive lysine, arginine or methionine, were each digested with trypsin and the tryptic peptides were separated by column chromatography on Bio-Rad cation exchanger, Aminex A-5. The tryptic peptide pattern of the wild type enzyme was compared with the tryptic peptide pattern of the enzyme from each mutant cell line. The enzyme from the wild type cells was composed of a minimum of 10 lysine- and 8 arginine-containing tryptic peptides in addition to the COOH-terminal peptide, identified as a methionine-containing tryptic peptide. The tryptic peptide patterns of the RJK3 and RJK39 enzymes differed from the tryptic peptide of the wild type in one lysine containing peptide. The COOH-terminal tryptic peptides of both RJK3 and RJK39 enzymes were unaltered. The lysine-containing peptide which could not be detected in the RJK39 enzyme preparation, reappeared when the enzymes were isolated from 3 revertants of RJK39. Based upon these findings, these investigators concluded that RJK3 carries either a missense or deletion mutation and RJK39 carries a missense mutation in the structural gene for HG-PRTase.

The susceptibility of mammalian cells to malignant conversion by chemical agents in-vivo is increased during replication. Tong et al (66) examined the question of whether mammalian cells have different susceptibilities to the mutagenic effects of chemicals during the cell growth cycle. They used two distinct cell synchronization procedures, one a nontoxic serum deprivation technique and the other a double thymidine block to obtain rat liver epithelial cells in different phases of the cell cycle. They then exposed these cells to the chemical mutagens/ carcinogens, methyl methanesulfonate and N-methyl-N'-nitro-N-nitrosoguanidine. They observed that the mammalian cells in the S phase were more susceptible to chemical mutagens than during other phases of the cell cycle. They suggested that the sensitivity of S-phase cells could be due to a lack of opportunity for the cell to repair DNA damage before the damaged regions are used as templates for the synthesis of new and therefore faulty DNA. Another reason could be that critical sites of the DNA are exposed to damage by mutagens during DNA synthesis in the S-phase.

Transport. The transport of exogenous purine and pyrimidine into yeast cells have been described as a function separate from phosphoribosylation (67,68). Evidence supporting this conclusion included the

identification of two purine permeases, an adenine permease and a guanine permease, both of which recognize hypoxanthine in Saccharomyces cerevisiae (69). The uptake of pyrimidines in Saccharomyces cerevisiae also occurs using at least two permeases, one permease is specific for cytosine and the other for uracil. The cytosine permease may also transport the purine bases adenine and hypoxanthine, since the growth behavior of purine-requiring mutants, as well as direct uptake measurements, showed that hypoxanthine uptake and adenine uptake were strongly depressed in a mutant of Saccharomyces cerevisiae lacking the cytosine permease (70). Also observed was a reduced uptake of purines in Saccharomyces mutant strains, which lacked the corresponding phosphoribosyltransferase activity (68). However, the reduction in the uptake of purines did not support the hypothesis of a group-translocation mechanism involving the phosphoribosyltransferase, but implied that the uptake of purines is mediated by a transport system and that uptake is facilitated if the intracellular purine base is removed by the corresponding phosphoribosyltransferase. Further evidence to support this assumption was supplied by studies on the transport of purines and pyrimidines in wild type Novikoff cells and HG-PRTase deficient Novikoff cells. These studies demonstrated that the transport of

purines and pyrimidines was facilitated by a carrier mediated transport system and that a decrease in the uptake of hypoxanthine and adenine reflected the substrate saturation of the respective phorphoribosyltransferases rather than of the transport system (71).

In contrast to these results, the transport of purine bases into microbial cells was described as a group translocation mediated by membrane-bound phosphoriboslytransferase (72). This conclusion was questioned by other investigators whose data suggested that the transport of purine bases across the bacterial membrane is a function separate from phosphoribosyltransferase activities (73,74). Evidence to support this concept was the recent isolation and characterization of two Salmonella typhimurium strains with defects in the uptake of purines (75). These defects in purine transport were distinct and separate from the corresponding purine phosphoribosyltransferase activity since both mutants possess phosphoribosyltransferase activities that were similar to those of the respective parental strains. One mutant (CB-3) showed a decrease in the rate of guanine uptake that was probably caused by a mutation in the specific gene (guaP) which mediated the transport of guanine. The other mutant (GP103) had a purine carrier molecule with an altered specificity and

showed a reversal of the parental uptake specificity. The uptake of [^{14}C]-hypoxanthine which normally is inhibited by the addition of unlabeled xanthine in the parental strain was unaffected by xanthine addition. These studies provided genetic evidence that purine uptake is mediated by a transport system which is separate from the phosphoribosyltransferase activity.

Rationale. As detailed in this section, HG-PRTase occupies a crucial position in the intermediary metabolism of every living cell, and an understanding of its function is important. The studies described in this thesis were initiated in order to define the kinetic mechanism of HG-PRTase from yeast to see if the sequence of substrate additions to this enzyme is similar to the sequence described for HG-PRTase from human erythrocytes or is similar to the Ping Pong BiBi kinetic mechanism through which yeast orotate phosphoribosyltransferase proceeds (76).

Alternate-substrate kinetic analysis was chosen as one of the methods for determining whether substrate addition to yeast HG-PRTase was sequential or non-sequential because we have devised an HPLC assay procedure, modified from the procedures of Vasquez and Bieber (77) and Hanna and Sloan (78) which allows IMP and GMP formations to be monitored simultaneously. We

reasoned that rate measurements using this procedure would allow us to test the sensitivity of our new method and to test the validity of the "one product" and "common product" theories for alternate-substrate kinetic analysis of Huang (79,80) as well as to determine the kinetic mechanism of the yeast HG-PRTase catalyzed reactions.

The use of bifunctional cross-linking reagents to obtain information about the stoichiometry of oligomeric proteins has been previously discussed by Davies and Stark (81). Bifunctional imidoesters have proved to be valuable reagents for probing protein-protein interactions (82,83) and the technique of chemical cross-linking has been extended to study the topology of protein association in such complex systems as ribosomes and the geometrical arrangement of peptides in biological membranes (84,85). Chemical cross-linking of HG-PRTase with bifunctional imidoesters with subsequent denaturation and separation by sodium dodecylsulfate polyacrylamide gel electrophoresis was employed to study the subunit structure of HG-PRTase.

THEORY OF CROSS-LINKING

Chemical modification of specific amino acid side chains of proteins is an extremely useful tool to the protein chemist. Several methods are available that have a high specificity for modifying or blocking either the carboxyl group or the amino group of proteins. The carbodiimide-nucleophile procedure is used for the modification of carboxyl groups (86). The charge on the carboxyl group depends on the nature of the nucleophilic reagent employed and could either be retained, or replaced by positive charges or eliminated. Lysine derivatives can also be prepared in which the positive charges on the lysine residues are retained (amidination), are eliminated (carbamylation), or are replaced by negative charges (maleylation). For the amidination of lysine residues, imidoesters are employed. Imidoesters are highly specific reagents for amino groups in proteins, they react with amino groups to form amidines, the reaction of which is analogous to the reaction of O-methylisourea with amino groups to form guanidines (87). In general, the amidination reaction can be written as shown in equation 6.

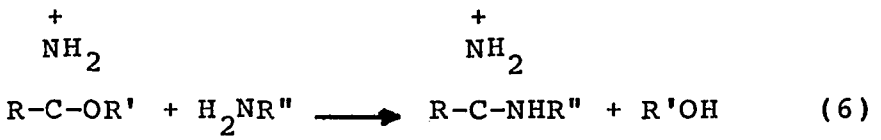

(6)

Diimidoesters of various chain lengths have been employed in the cross-linking of proteins. They react under mild conditions to yield derivatives with unaltered charges. A moderately high pH value is chosen in order to favor amidination reaction over hydrolysis of the diimidoester, since the ratio (k amidination/k hydrolysis) increases with increasing pH over the range of pH 7.5 to pH 10. The optimum pH for cross-linking of protein subunits with these reagents is pH 8.5 (81). Under appropriate conditions (low protein concentrations) cross-linking between oligomers is not significant, whereas these reactions have been found to occur at high protein concentrations. At low protein concentration cross-linking within the oligomer is unaffected. Therefore amidination at different protein concentrations can be used as a test by which cross-linking between oligomers and cross-linking within an oligomer can be distinguished. Cross-linking within an oligomer may occur

within each chain, or between chains. Another possibility is monofunctional modification, followed by hydrolysis of the other end of the diimidoester to form an ester (88). When these modified proteins are denatured, only the proteins with covalent links between chains will have different molecular weights from that of the monomer, the difference of which can be resolved by sodium dodecylsulfate gel electrophoresis.

The mechanism of cross-linking by the diimidoesters and glutaraldehyde is similar. In both cases the ϵ-amino group of the lysyl residues are involved. Glutaraldehyde forms a Schiff base with the amino groups and the diimidoesters react with the amino groups to form amidines. The structures of glutaraldehyde and dimethylsuberimidate as well as their reactions with the lysyl residues of proteins are shown in Figure 2.

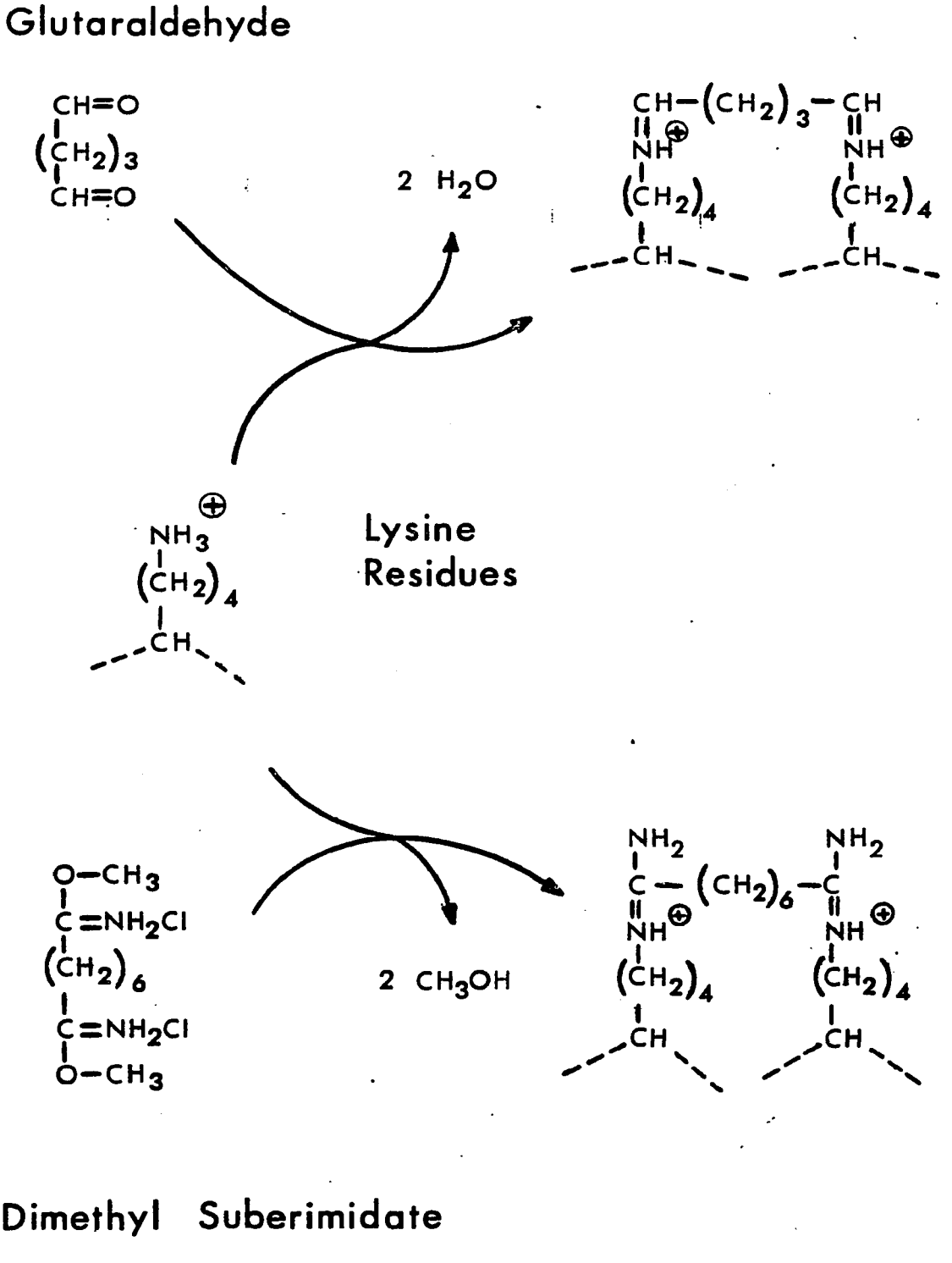

Figure 2. Cross-linking reactions

MATERIALS AND METHODS

Materials. Bakers' yeast (Budweiser brand) was obtained from Valenti Yeast, Inc., Flushing, N.Y. PRibPP (sodium salt), hypoxanthine, guanine, IMP, GMP, acrylamide, dimethyl suberimidate, triethanolamine, egg albumin, bovine serum albumin, trypsinogen and lysozyme were purchased from Sigma Chemical Co., (St. Louis). N,N'-methylenebisacrylamide, N,N,N',N'-tetramethylenediamine and sodium dodecylsulfate were supplied by Bio-Rad (Richmond, CA). AH-Sepharose-4B, Sephadex G-100, ribonuclease A, chymotrypsinogen A, ovalbumin, aldolase and Blue Dextran 2,000 were obtained from Pharmacia Fine Chemicals (Piscataway, N.J.). [8-^{14}C]-guanine, [8-^{14}C]-hypoxanthine and [^{32}P]-pyrophosphate were supplied by New England Nuclear (Boston, Mass.). All other chemicals were reagent grade. [1-^{14}C]-PRibPP was synthesized from [1-^{14}C]-ribose using ribokinase and PRibPP synthetase activities obtained from Salmonella typhimurium grown on a ribose-rich medium. Labeled PRibPP was isolated using DEAE-cellulose, charcoal treatment and DBAE-cellulose, the detailed procedures for which have beem described previously (89). Excess salt was removed from this radioactive sample by elution through G-10 Sephadex and lyophilization was employed to concentrate the radioactivity.

Enzyme Purification. Hypoxanthine-guanine phosphoribosyltransferase was purified from Saccharomyces cerevisiae by methods described below, which are adaptions of several literature procedures (3,11). All procedures were performed at 4°C.

1) 10 lbs of Bakers' yeast were added to 2200 ml of toluene previously brought to 45°C and the mixture was incubated in a 45°C water-bath for 90 min. with occasional stirring. The suspension was removed from the water-bath and left to stand at room temperature until the foaming action ceased (approx. 2 hrs.). 5 liters of precooled double distilled water were added and the mixture was stirred a few times, then allowed to stand at 4°C overnight in order to effect separation of the organic phase from the aqueous phase. The opaque aqueous mixture was collected and clarified by centrifugation (12,000 rpm for 25 min.).

2) This supernatant was brought to 50 mM $MnCl_2$ concentration, and allowed to stand at 4°C overnight to precipitate nucleic acid material, which was removed by centrifugation (12,000 rpm for 25 min.).

3) The supernatant from the $MnCl_2$ treatment was brought to 60% saturation with ammonium sulfate and stirred overnight. The resulting precipitate was removed by

centrifugation, dissolved in 50 mM Tris-HCl buffer (pH 7.5) containing 10 mM $MgCl_2$, 1mM dithiothreitol and 15% glycerol and dialysed against 16 liters of the same buffer for 6 hours with one change of buffer.

4) 100 ml aliquots of the dialysed enzyme solution were incubated at 70°C for 5 min. with continuous stirring then quickly cooled by placing in an ice-bath. The denatured protein was removed by centrifugation at 16,000 xg for 30 min. The supernatant was collected and stored at -76°C.

5) A GMP-Sepharose column (2x29 cm) was prepared according to the method of Hughes et al (3) using the modifications made by Schmidt et al (11). 50 ml aliquots of the heat treated fraction were applied slowly to the GMP-Sepharose column (flow rate of 2 drops/min.). The column was washed with 50 mM Tris-HCl (pH 7.5) containing 10 mM $MgCl_2$, 1.2 M KCl, 15% glycerol and 1mM dithiothreitol to remove any unattached protein. Then, hypoxanthine-guanine phosphoribosyltransferase was eluted with the same buffer which contained 5 mM GMP, a procedure first described by Gutensohn et al (90). The fractions containing the HG-PRTase activity were pooled and concentrated by using an Amicon ultrafiltration apparatus and a PM-10 membrane. GMP was completely removed from

the enzyme solution after three successive concentration steps with a solution containing 50 mM Tris-HCl, 10 mM $MgCl_2$, 15% glycerol and 1mM dithiothreitol. The resulting enzyme solution was stored at -76°C for 6 months with no loss of enzymatic activity.

Gel Electrophoresis. Polyacrylamide gel electrophoresis was performed with 7.5% polyacrylamide at room temperature at several pH values (7.0, 8.0, and 9.0) according to the method of Davis (91).

Isoelectricfocusing. Isoelectricfocusing was performed at 4°C in a 7.5% polyacrylamide gel with a pH gradient from pH 3 to pH 10 according to the method of Wrigley (92). 15 ug of enzyme was applied to the gradient. At the end of the run, one gel was cut into 2 mm slices, which were placed in a small test-tube (12x75 mm) containing 1ml of distilled H_2O and their pH values were measured.

Molecular Weight Determination. The native molecular weight of HG-PRTase was estimated by comparison of its elution volume from a Sephadex G-100 column with that of 5 proteins of known molecular weights: aldolase (m.w. 158,000), bovine serum albumin (m.w. 66,000), ovalbumin (m.w. 45,000), chymotrypsinogen A (m.w. 25,000), and ribonuclease A (m.w. 13,700). The column was equilibrated with a 50 mM Tris-HCl, buffer (pH 7.5) containing 10 mM $MgCl_2$, 20 mM KCl and 1 mM

dithiothreitol. The proteins were eluted with the same buffer at a flow rate of 15 ml/hr. 4.7 ml fractions were collected and aldolase, bovine serum albumin, ovalbumin, chymotrypsinogen A and ribonuclease A were detected in the effluents by measurement of the absorbance at 280 nm using a Perkin Elmer Recording vis/uv Spectrophotometer (Model 101). The HG-PRTase peak was identified through the use of the assay procedure described in "Methods".

Cross-Linking Studies. Chemical cross-linking of HG-PRTase was accomplished utilizing the bifunctional reagents, dimethylsuberimidate (81) and glutaraldehyde (93). 200 ul aliquots of HG-PRTase (0.27 mg/ml) in 50 mM triethanolamine buffer, pH 8.5, were added to a freshly prepared 2% solution of glutaraldehyde in 0.2 M triethanolamine buffer, pH 8.5. The reactions were allowed to proceed at room temperature for either 30 sec or 30 min. Thereafter the reactions were terminated by freezing the solutions in a dry-ice/acetone bath. The experiment was repeated with enzyme that was pretreated with 1 mM PRibPP at 4°C for 20 min.

Immediately before use, a 5 mg/ml dimethylsuberimidate solution in 0.2 M triethanolamine buffer, pH 8.5 was prepared. 200 ul aliquots of enzyme (0.27 mg/ml) in 50 mM triethanolamine buffer, pH 8.5 were incubated with 30 ul

of this solution for 4 hr. at room temperature. The experiment was repeated with enzyme that was preincubated with 1 mM PRibPP at 4°C for 20 min. Samples of these reaction mixtures were stored at -76°C for later use in the electrophoresis experiments.

Sodium Dodecylsulfate Polyacrylamide Gel Electrophoresis. The subunit molecular weight of HG-PRTase was determined by sodium dodecylsulfate (SDS) gel electrophoresis according to the procedure of Laemli (94).

The electrophoretic buffer contained 3 g Tris, 14.4 g glycine and 1 g SDS per liter of solution. The separating gel consisted of 10% acrylamide with 0.8% N'N'-methylenebisacrylamide in 0.608 Tris-HC1 buffer, pH 8.8 with 0.16% SDS. The stacking gel consisted of 3% acrylamide in 0.147 M Tris-HC1 buffer, pH 6.8 containing 0.12% SDS. The glass tubes used were 10 cm long with an inner diameter of 5 mm. Each tube was filled with 2 ml of separating gel and 0.5 ml of stacking gel was layered on the top. Unmodified samples of HG-PRTase as well as samples that were previously treated with glutaraldehyde and dimethylsuberimidate were mixed with a 0.0625 M Tris-HC1 buffer, pH 6.8 containing 2% SDS, 10% glycerol, 5% β-mercaptoethanol and 0.001% Bromphenol blue. These samples were denatured by placing them in a boiling

water-bath for 1 min. The denatured protein solutions were then applied onto the gels and electrophoresis was performed at a constant current of 3 ma per gel until the dye marker approached the end of the tube. The gels were removed, cut at the dye band, stained overnight with 0.05% Coomassie blue and destained with 7% acetic acid (95).

High Pressure Liquid Chromatography. A Waters HPLC Instrument equipped with a Model 6000A solvent delivery system, Model U6K sample injector, Model 440 absorbance detector, and a Houston Omniscribe chart recorder was used in the assay procedure. A single Brownlee MPLC ion-exchange column (equilibrated with 0.5 M phosphate, pH 4.0) was placed on-line with the solvent delivery system at a flow rate of 2 ml/min. 10 ul samples were injected using a Hamilton 801 microliter syringe, and eluted with 300 - 500 psi pressure. Nucleotides and/or bases in the eluent were detected at 254 nm using a 0.05 absorbance setting. Impurities in the solvents used in these chromatographic runs were removed by vacuum filtration through a 0.45 mm HA Millipore filter.

Enzyme Assay. Measurements of the initial velocities of the hypoxanthine-guanine phosphoribosyltransferase reactions were accomplished using a modification of the method described by Flaks (96). The assay mixture

consisted of 0.2 ml hypoxanthine or guanine (54 uM final concentration), 0.4 ml PRibPP (100 uM), 0.1 ml $MgCl_2$ (1.0 mM) and 0.1 ml potassium phosphate buffer, (25 mM, pH 7.4) in a final volume of 2.4 ml. The mixture was placed in a 38°C water-bath and the reaction was initiated by the addition of 1.6 ml of dilute enzyme solution. The reaction was terminated at an appropriate time period by heating the samples in a boiling water-bath for 1 min. Denatured protein was removed by centrifugation and the supernatant was filtered through a 0.45 mm HA Millipore filter prior to HPLC injection.

Isotope Exchange Studies. The reaction mixture consisted of 0.2 ml of [8-^{14}C] hypoxanthine or guanine (0.05 mCi, 1mM) 0.4 ml IMP or GMP (1mM), 0.1 ml $MgCl_2$ (10 mM), 0.1 ml potasium phosphate buffer (0.25 M, pH 7.4) and 1.6 ml of enzyme solution (71 ug). The mixture was incubated at room temperature for 15 min. and the incubation was terminated by placing the sample in a boiling water bath for 1 min. Denatured protein was removed by centrifugation and the supernatant was filtered through a 0.45 mm HA Millipore filter prior to HPLC injection. Separation of substrates and products (hypoxanthine and IMP or guanine and GMP) was achieved by HPLC using a Waters C_{18}-Bondapak column, and an aqueous 10% methanol

solution was employed to elute bases and nucleotides. The fractions containing base and nucleotide were collected separately and tested for radioactivity using a Beckman LS-150 liquid scintillation counter.

Studies of the HG-PRTase catalyzed exchange of label between [^{32}P]-pyrophosphate and PRibPP were performed using techniques described by Victor et. al. (76).

Flow Dialysis. The dialysis cell (Technilab) consisted of an upper and lower chamber separated by a membrane made from commercially available dialysis tubing. Buffer solution (10 mM sodium phosphate, pH 7.4) was pumped through the lower chamber at a constant rate (4 ml/min.). The lower chamber was attached to a fraction collector and 3 ml fractions were collected. Aliquots of 0.5 ml from each fraction were added to 3.0 ml of Bray's solution and the radioactivity was measured using the Beckman liquid scintillation counter.

Binding studies were performed as described by Colowick and Womack (97). Initially [1-^{14}C]-PRibPP (sp. act. = 1000 cpm/ug) was added to 1.4 x 10^{-5}M hypoxanthine-guanine phosphoribosyltransferase in the upper chamber. This labeled PRibPP was allowed to equilibrate with the enzyme at 4°C and thereafter 10 ul samples of unlabeled PRibPP were added to the enzyme

solution in order to establish a new steady-state level. Increments of unlabeled PRibPP ranging in concentration from 7.5×10^{-6} to 5×10^{-2}M were employed to determine steady-state concentrations of PRibPP solution across the membrane. Analogous non-enzymatic studies were also carried out.

The above experiments were repeated using [8-^{14}C]-guanine (specific activity 6.03 mCi/mMol) and unlabeled guanine (8×10^{-5} to 2.2×10^{-3}M), and using [8-^{14}C]-hypoxanthine (specific activity 55.3 mCi/mMol) and unlabeled hypoxanthine (8×10^{-5} to 2.2×10^{-3}M). The enzyme concentration was 1.4×10^{-5}M. These experiments were performed at room temperature.

RESULTS

HG-PRTase Subunit Structure Determination. HG-PRTase was purified from yeast using procedures modified from those described previously (3,11,Table I). A partially purified preparation (after heat treatment) was stored at -76°C until pure enzyme was required. Then 50 ml aliquots of the heat treated preparation was applied directly to the affinity column. This procedure yielded a homogeneous HG-PRTase solution as determined by the criteria of polyacrylamide gel electrophoresis. An elution profile of the HG-PRTase from the GMP-Sepharose column is illustrated in Figure 3. The enzyme was bound to the column in a high ionic strength buffer, no activity was removed during the initial wash with a buffer containing 1.2 M KCl. The addition of 5 mM GMP to the starting buffer facilitated the elution of the HG-PRTase which eluted with the leading edge of the GMP peak. Figure 4 illustrates the successive progress of the purification of HG-PRTase by this method. Isoelectricfocusing of the purified enzyme showed one peak of enzyme activity with an isoelectric pH value of 6.85 (Figure 5). Only purified enzyme was utilized in the studies described below.

TABLE I

Purification of HG-PRTase from Baker's Yeast

Solution	Vol.(ml)	Prot.(mg)	Act.[a]	Sp.Act.[b]	Purity
Extract	6500	27,300	2.4	0.57	-
$MnCl_2$ Treatment	6240	17,470	0.8	0.29	-
$(NH_4)_2SO_4$ Fract.	800	10,710	11.4	0.85	1.8
Heat Treatment	750	6,720	10.4	1.16	2.5
Affinity Chromatography	10	5.4	205	379	6,650

a) Units of nmoles GMP/min/ml solution

b) Units of nmoles GMP/min/mg protein

Figure 3. Elution profile of HG-PRTase from GMP-Sepharose affinity column. An affinity column (2 x 29 cm) was loaded with 50 ml of 70°C heat treated fraction at a flow rate of 2 drops per min. The column was washed and HG-PRTase was eluted as described in "Methods". Absorbance at 280 nm (—●—●—). HG-PRTase activity (—△——△—).

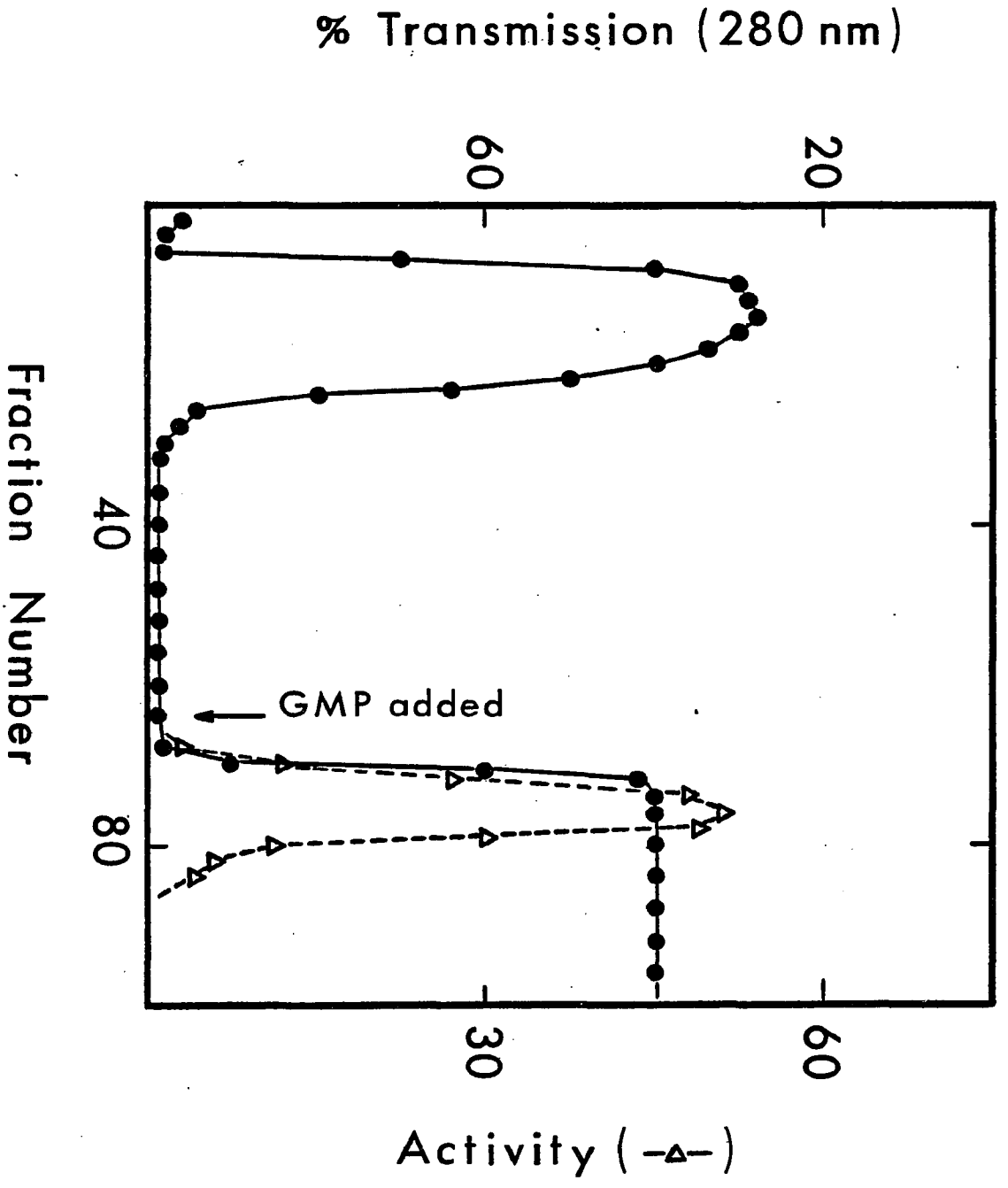
% Transmission (280 nm)
60
20
Fraction Number
40
80
GMP added
30
60
Activity (-Δ-)

Figure 4. Polyacrylamide gel electrophoresis runs of HG-PRTase samples A) after ammonium sulfate fractionation, B) after 70°C heat treatment and C) after GMP-Sepharose chromatography. Conditions for these experiments were described in "Methods".

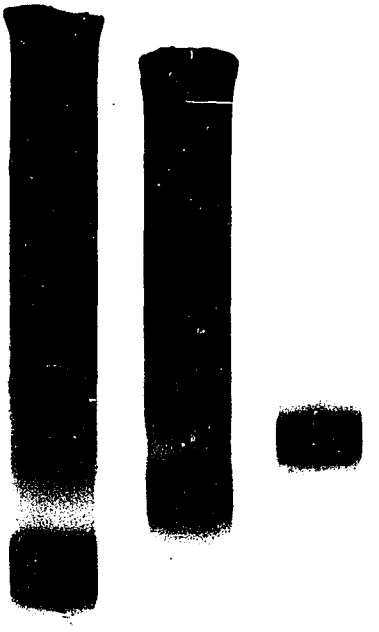

A B C

The molecular weight of the native enzyme was determined by Sephadex G-100 column chromatography which was calibrated with proteins of known molecular weights. The enzyme eluted in a single peak just ahead of the ovalbumin and behind the bovine serum albumin peak corresponding to a molecular weight of approximately 52,000 (Figures 6A and 6B). The subunit molecular weight of the purified enzyme was also investigated by sodium dodecylsulfate polyacrylamide gel electrophoresis. HG-PRTase migrated as a single band. When the mobility of this band was compared with the mobility of proteins with known molecular weights, the subunit molecular weight of HG-PRTase was calculated to be about 26,000 (Figure 7).

Chemical cross-linking studies with bifunctional reagents were employed to investigate the subunit structure of HG-PRTase. The purified enzyme was cross-linked with glutaraldehyde according to the method of Kapoor and O'Brien (93). The results of cross-linking and subsequent sodium dodecylsulfate polyacrylamide gel electrophoresis are shown in Figure 8A. Only one band corresponding to the monomer (m.w. 26,000) was observed with the unmodified enzyme, while two major bands could be seen for the cross-linked enzyme; one band originating from cross-linked subunits and corresponds to the dimer

Figure 5. Results of isoelectricfocusing of HG-PRTase performed in a 7.5% polyacrylamide gel from pH 3 to pH 10 as described in "Methods". A) pH profile of one gel with position of HG-PRTase (▶) activity denoted. B) Absorbance (280 nm) scan of a duplicate gel.

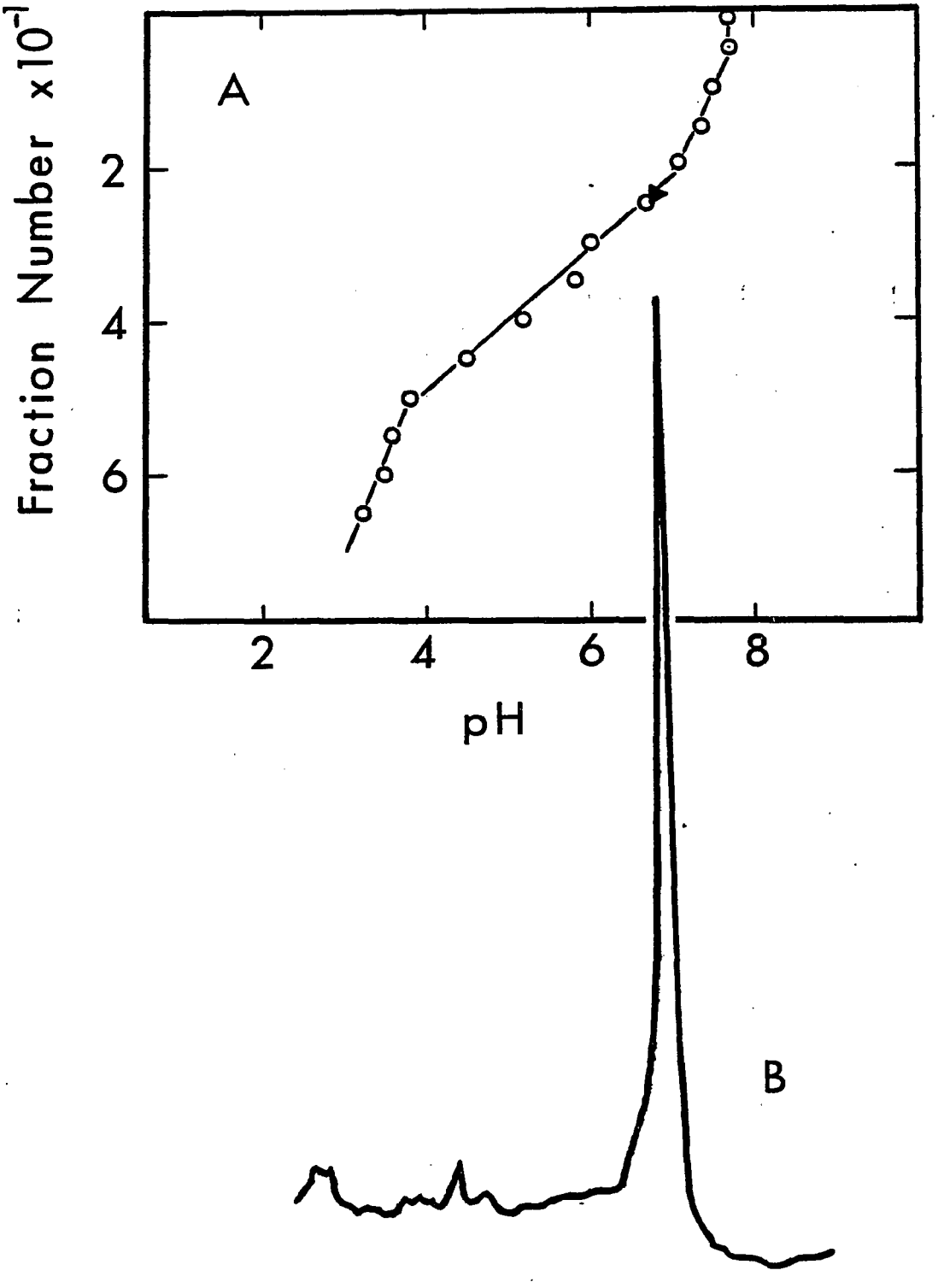
Fraction Number x10⁻¹
A
2
4
6
2
4
6
8
pH
B

Figure 6. A) Determination of the native molecular weight of HG-PRTase by gel filtration on Sephadex G-100 column (2x100 cm). 50 ug of HG-PRTase and 5 mg/ml of each standard were applied successively to a Sephadex G-100 column which was previously equilibrated with 50 mM Tris-HCl buffer, pH 7.5 containing 10 mM $MgCl_2$, 20 mM KCl and 1 mM dithiothreitol. Absorbance at 280 nM (—o— , —●—) as well as enzyme activity (—Δ—) are illustrated. The void volume of the column determined by the elution of Blue Dextran 2000 was 108.1 ml. The molecular weights of the standards are: a) aldolase, 158,000; b) bovine serum albumin, 66,000; c) ovalbumin, 45,000; d) chymotrypsinogen A, 25,000; e) ribonuclease A, 13,700. B) Plot of molecular weight versus elution profile for standard proteins and HG-PRTase.

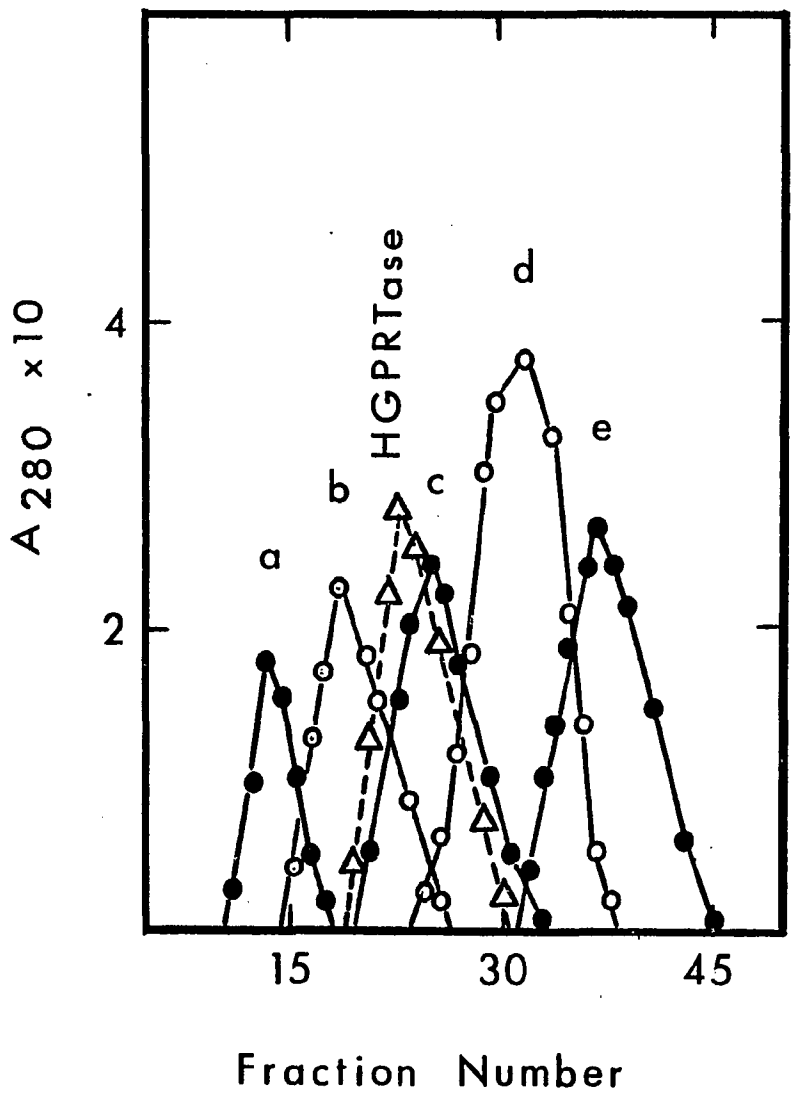
A 280 x10
4
2
15
30
45
Fraction Number
HGPRTase
a
b
c
d
e

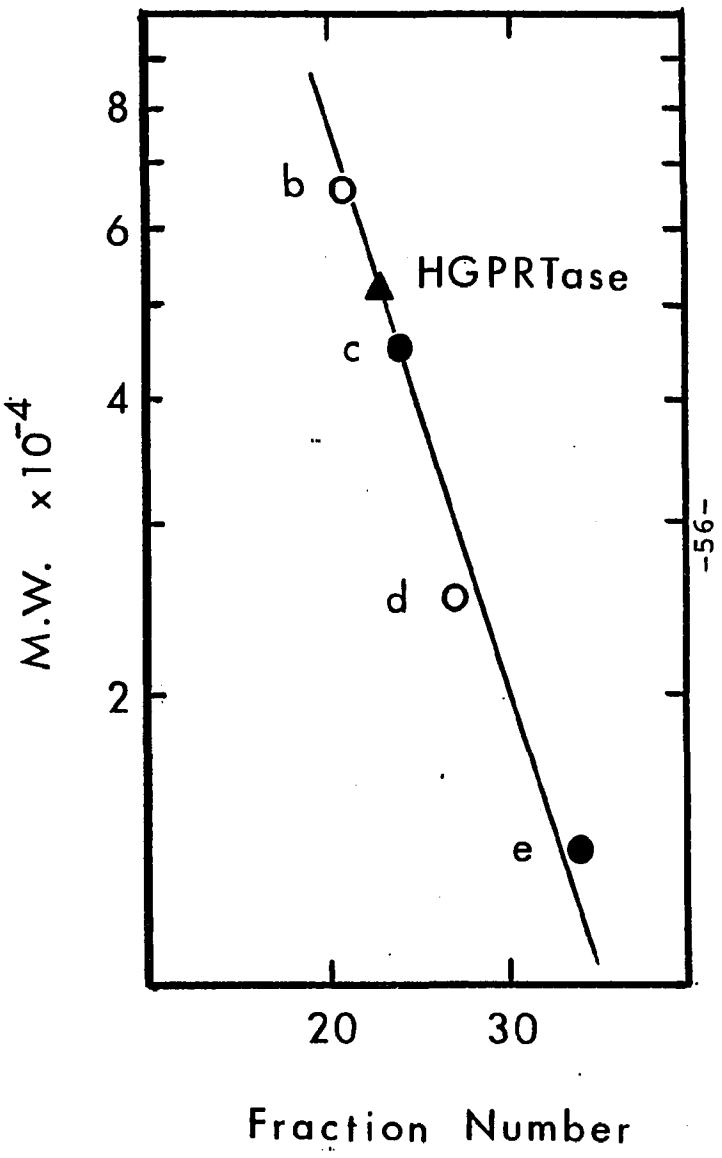
M.W. x10⁻⁴
8
6
4
2
20
30
Fraction Number
HGPRTase
b
c
d
e

Figure 7. Subunit molecular weight determination by sodium dodecylsulfate gel electrophoresis. Electrophoresis was carried out on a 10% polyacrylamide gel as described in "Methods". The standards used were: a) bovine serum albumin (m.w. 66,000); b) egg albumin (m.w. 45,000); c) pepsin (m.w. 35,000); d) trypsinogen (m.w. 24,000) and e) lysozyme (m.w. 14,000). The position of the single stained band of HG-PRTase is denoted by the closed triangle.

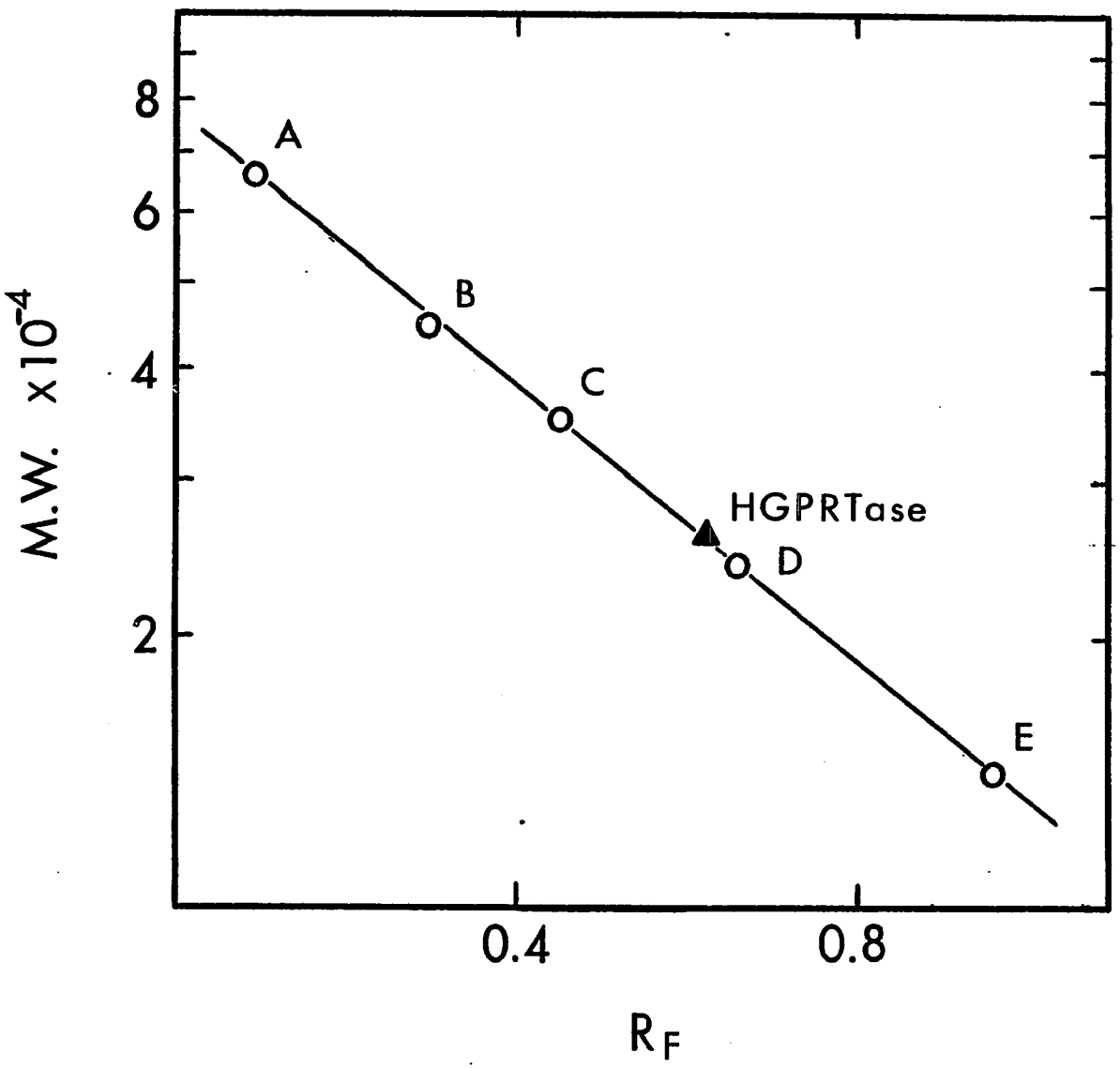
8
6
4
2
M.W. x10⁻⁴
A
B
C
HGPRTase
D
E
0.4
0.8
R_F

and the other from free uncross-linked subunits corresponding to the monomer. These two protein species were present in both the 30 sec. cross-linking reaction time and after the 30 min. incubation period. A plot of the logarithm of the molecular weight of each cross-linked protein species against the corresponding mobility is shown in (Figure 8B). The points fall on a straight theoretical curve generated from multiples of 26,000 molecular weight. This confirms that the protein species produced by cross-linking are multiples of the monomer and suggests that the enzyme is a dimer composed of two identical or similar subunits. Preincubation of the enzyme with Mg-PRibPP before the cross-linking experiment showed no significant change in the pattern. Similar results were obtained for the human erythrocyte enzyme and the beef brain enzyme (9,12). The amount of enzyme activity remaining after cross-linking with glutaraldehyde is shown in Table II.

The subunit structure of HG-PRTase was investigated further by cross-linking studies with dimethylsuberimidate. The results of cross-linking and sodium dodecylsulfate polyacrylamide gel electrophoresis are shown in Figure 9A. In contrast to the results observed with glutaraldehyde, several protein species were present. In order to deter-

Figure 8. A) Sodium dodecylsulfate gels of HG-PRTase cross-linked with glutaraldehyde. a) uncrosslinked HG-PRTase, b) HG-PRTase cross-linked with glutaraldehyde for 30 sec. in the presence of Mg-PRibPP, c) HG-PRTase cross-linked with glutaraldehyde for 30 min., d) HG-PRTase cross-linked with glutaraldehyde for 30 min. in the presence of Mg-PRibPP, e) HG-PRTase cross-linked with glutaraldehyde for 30 sec. B) Plot of the logarithm of the molecular weight versus the mobility for the covalently linked species produced by cross-linking HG-PRTase with glutaraldehyde.

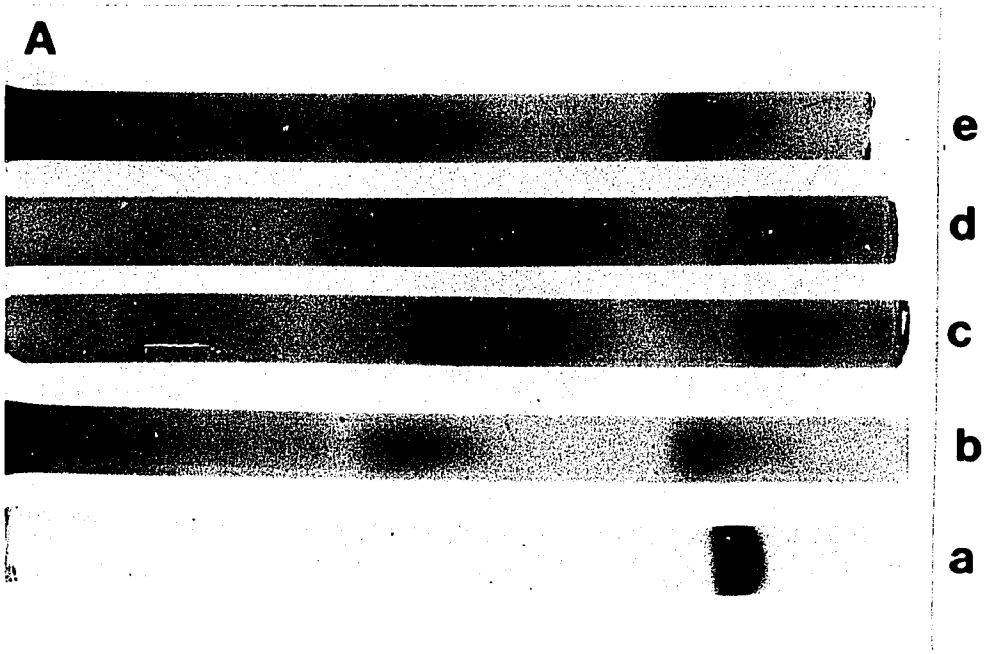
A
e
d
c
b
a

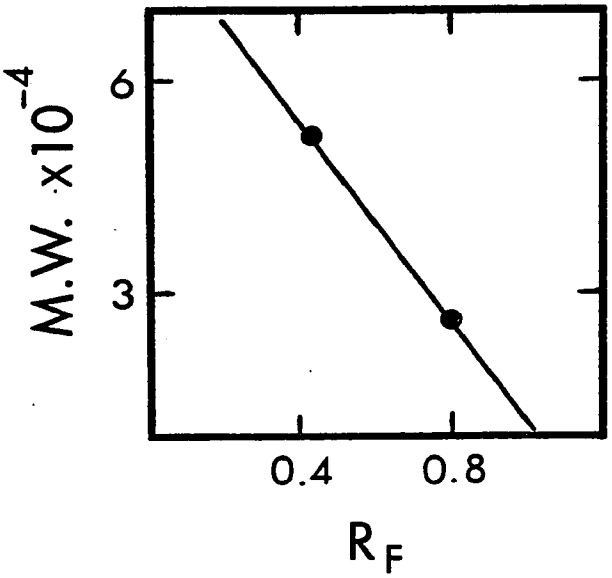
M.W. x10^{-4}
6
3
0.4
0.8
R_F

mine whether the molecular weights of these species were integral multiples of the monomer, the logarithm of the molecular weight of each specie was plotted against the corresponding electrophoretic mobility. A molecular weight of 26,000 was calculated for the monomeric species from a standard graph constructed from proteins of known molecular weights that were simultaneously subjected to electrophoresis with the cross-linked enzyme (Figure 7). As shown in Figure 9B, only band 4 corresponding to the dimer falls on this straight line. The other bands are not integral multiples of the monomer and do not fall on this straight line. These results suggest that the yeast HG-PRTase exists as a dimer and not as a trimer or tetramer. The expected molecular weights of the monomer, dimer, trimer and tetramer would be 26,000, 52,000, 78,000 and 104,000 respectively. Similar results were observed when the beef brain HG-PRTase was cross-linked with dimethylsuberimidate (12). These investigators found several bands, only three of which fell on a straight line and corresponded to monomer, dimer and trimer species. Preincubation of the enzyme with Mg-PRibPP did not affect the banding pattern. These results are in agreement with the results obtained for the human erythrocyte enzyme and the beef brain enzyme (9,12). The amount of enzyme activity

TABLE II

HG-PRTase activity after cross-linking with glutaraldehyde and dimethylsuberimidate

Conditions	% HG-PRTase Activity
No additions	100
1mM Mg-PRibPP + 2% Glutaraldehyde (30 sec.)	2
2% Glutaraldehyde (30 sec.)	2
1mM Mg-PRibPP + 2% Glutaraldehyde (30 min.)	2
2% Glutaraldehyde (30 min.)	< 1
1mM Mg-PRibPP + 5mg/ml Dimethylsuberimidate (4 hr.)	20
5mg/ml Dimethylsuberimidate (4 hr.)	7

Figure 9. A) Sodium dodecylsulfate gels of HG-PRTase cross-linked with dimethylsuberimidate. a) uncrosslinked enzyme, b) HG-PRTase cross-linked with dimethylsuberimidate in the presence of mg-PRibPP, and c) HG-PRTase cross-linked with dimethylsuberimidate. B) Plot of the logarithm of the molecular weight versus the mobility for the covalently linked species produced by cross-linking HG-PRTase with dimethylsuberimidate. Multiples of 26,000 are shown in filled circles.

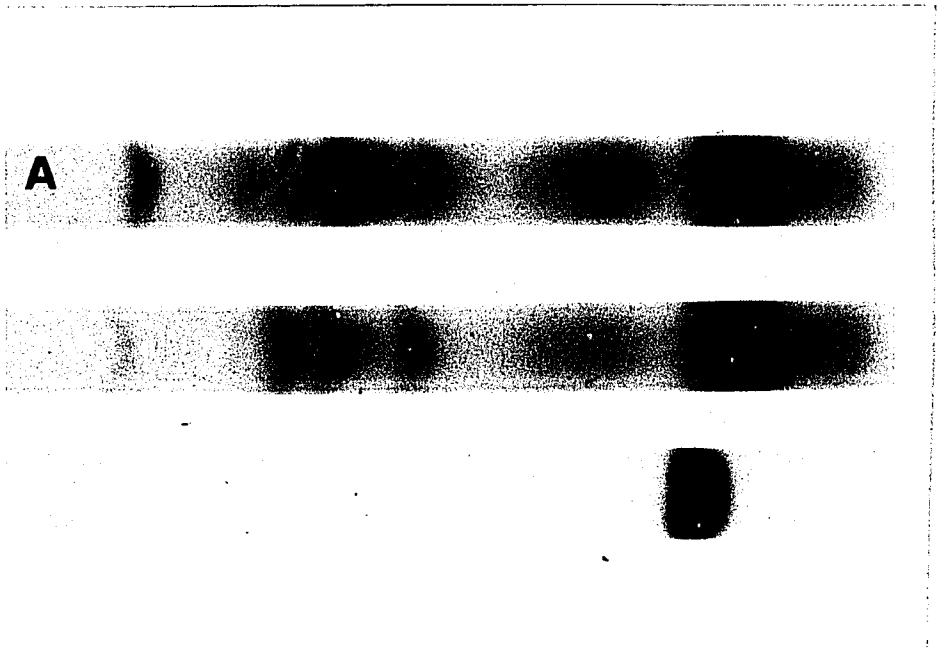
A
c
b
a

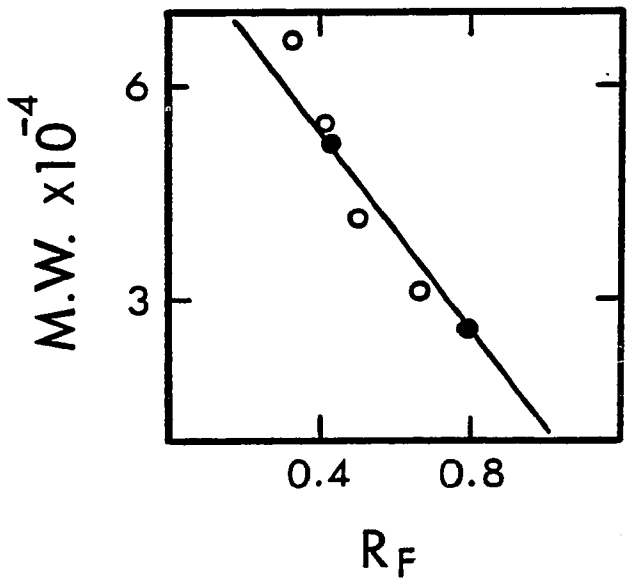
M.W. x10^{-4}
6
3
0.4
0.8
R_F

remaining after cross-linking with dimethylsuberimidate is shown in Table II.

Kinetic Analysis. The observation has been made that ion-exchange columns and HPLC can provide a complete separation of guanine, hypoxanthine, IMP and GMP, under appropriate conditions (Figure 10), from injected samples containing uM concentrations of all four components. Since the absorbance (254 nm) of each reactant in the elution profile is directly proportional to its solution concentration (Figure 11), this separation by ion exchange HPLC provides a means for monitoring the changes in concentration of nucleotides and bases during the course of the HG-PRTase-catalyzed reaction which is as sensitive as the reverse phase-HPLC procedure first described by Vasquez and Beiber (77). More importantly, however, the new procedure allows simultaneous evaluations of the HG-PRTase catalyzed formations of IMP and GMP and the effects of the presence of an alternate substrate on each reaction.

Three types of kinetic analyses were accomplished using the HPLC assay procedure: 1) The initial velocities of enzymatic IMP formation and GMP formation were monitored separately, in the presence of PRibPP and the appropriate base in the incubation mixture. 2) The initial velocities of these reactions were characterized simultaneously in

Figure 10. High pressure liquid chromatography elution profiles of an incubation mixture made up of 2 nmoles HG-PRTase, 50 uM guanine (G), 50 uM hypoxanthine (H), 100 uM PRibPP and 1mM $MgCl_2$ in potassium phosphate (pH 7.4). At time intervals (0-5 min.) aliquots of the mixture were injected onto the MPLC ion-exchange column and eluted using conditions described in "Methods". The insert in this figure illustrates the time-dependent utilizations of H and G and formations of GMP and IMP as determined by the absorbance of each peak at 254 nm.

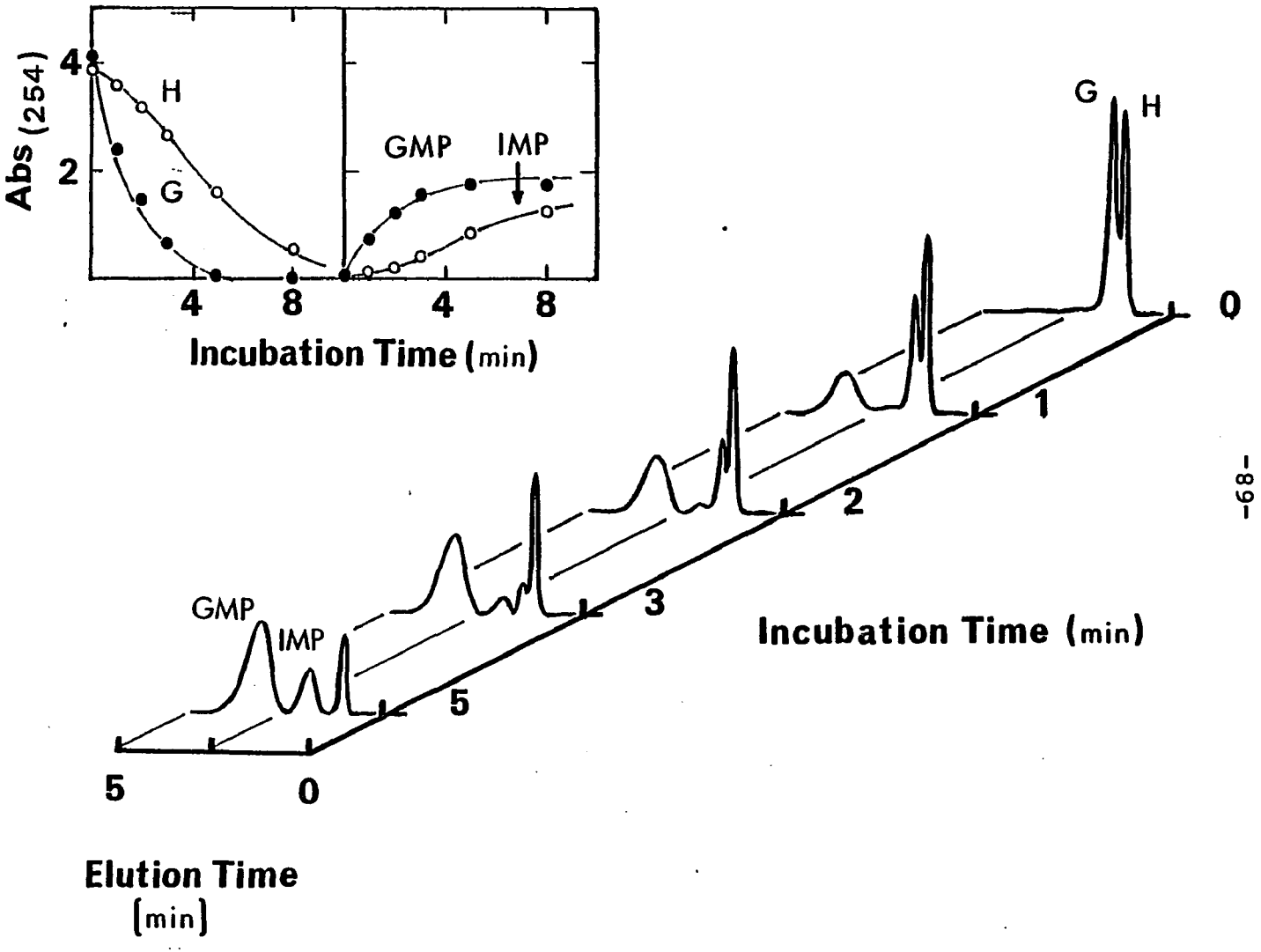
Abs (254)
4
2
H
G
GMP
IMP
4
8
4
8
Incubation Time (min)
G
H
0
1
2
3
5
GMP
IMP
5
0
Incubation Time (min)
Elution Time
(min)

Figure 11. Relationships between the assigned amplitudes of the absorbance (254 nm) peaks from the HPLC elution profile and the concentrations of injected standard solutions of IMP, GMP, hypoxanthine (H) and guanine (G). Standard solutions were injected and eluted through the ion-exchange column using conditions described in "Methods".

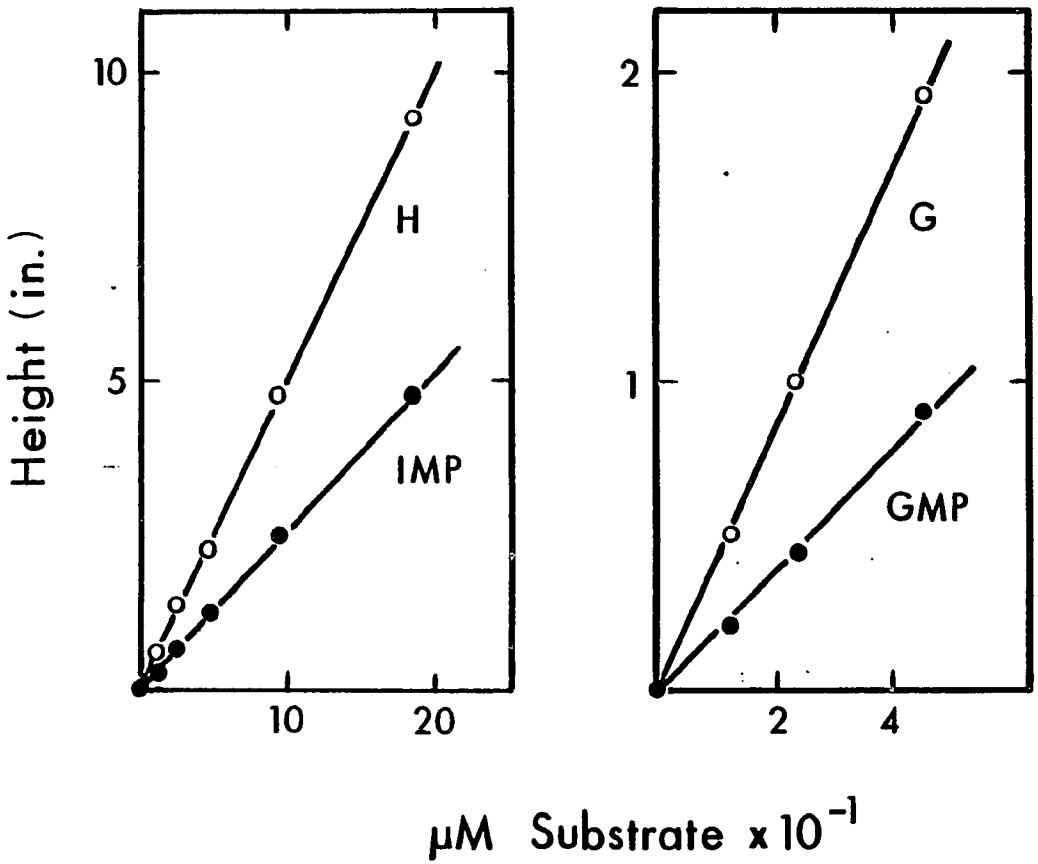
Height (in.)
10
5
H
IMP
10
20
2
1
G
GMP
2
4
μM Substrate x 10⁻¹

the presence of PRibPP and both bases. 3) The initial velocities of enzymatic PRibPP utilization (the common substrate) were measured in the presence of various fixed ratios of guanine and hypoxanthine. The latter two procedures made use of the same data.

As shown in Figure 12A and 12B, non-competitive patterns were observed when the reciprocal of the velocities of IMP formation were plotted against the reciprocal concentration of hypoxanthine in the presence of three concentrations of PRibPP (Figure 12A) and against the reciprocal concentration of PRibPP in the presence of six concentrations of hypoxanthine (Figure 12B). Similarly, non-competitive patterns were observed when the reciprocal of the velocities of GMP formation were plotted against the reciprocal concentration of guanine in the presence of three concentrations of PRibPP (Figure 12C) and against the reciprocal concentration of PRibPP in the presence of three concentrations of guanine (Figure 12D). These results suggest that HG-PRTase catalyzes both GMP and IMP formations through the use of a sequential kinetic mechanism. In order to determine the nature of this sequential mechanism, alternate-substrate kinetic analyses of these reactions, fashioned after the theory of Huang (79,80), were performed.

Figure 12. Double reciprocal plots of the initial velocity of nucleotide formation versus initial substrate concentrations as determined using the HPLC assay procedure for HG-PRTase. A) Reciprocal rate of IMP formation vs reciprocal hypoxanthine (H) concentration in the presence of 154 uM (bottom line), 77 uM (middle line) and 39 uM (top line) PRibPP. B) Reciprocal rate of IMP formation vs reciprocal PRibPP concentration. The following concentrations of H were employed (starting from the bottom line to the top): 186 uM, 92 uM, 46 uM, 23 uM, 12 uM, 6 uM. C) Reciprocal rate of GMP formation vs reciprocal guanine concentration in the presence of 154 uM (bottom line), 77 uM (middle line) and 39 uM (top line) PRibPP. D) Reciprocal rate of GMP formation vs reciprocal PRibPP concentration in the presence of 46 uM (bottom line), 23 uM (middle line) and 12 uM (top line) guanine. Each point represents an average of 2-16 initial velocities generated by monitoring the rate of reactant concentration changes over a 5 min. incubation period. The straight lines which fit these points were generated by weighting rates successively according to the varied substrate, with the rate at the highest substrate concentration given the most weight. The points of convergence of the line were then averaged and this point

Figure 12. (cont'd) was included in the generation of a second series of lines for the graph, again using the successive weighting procedure.

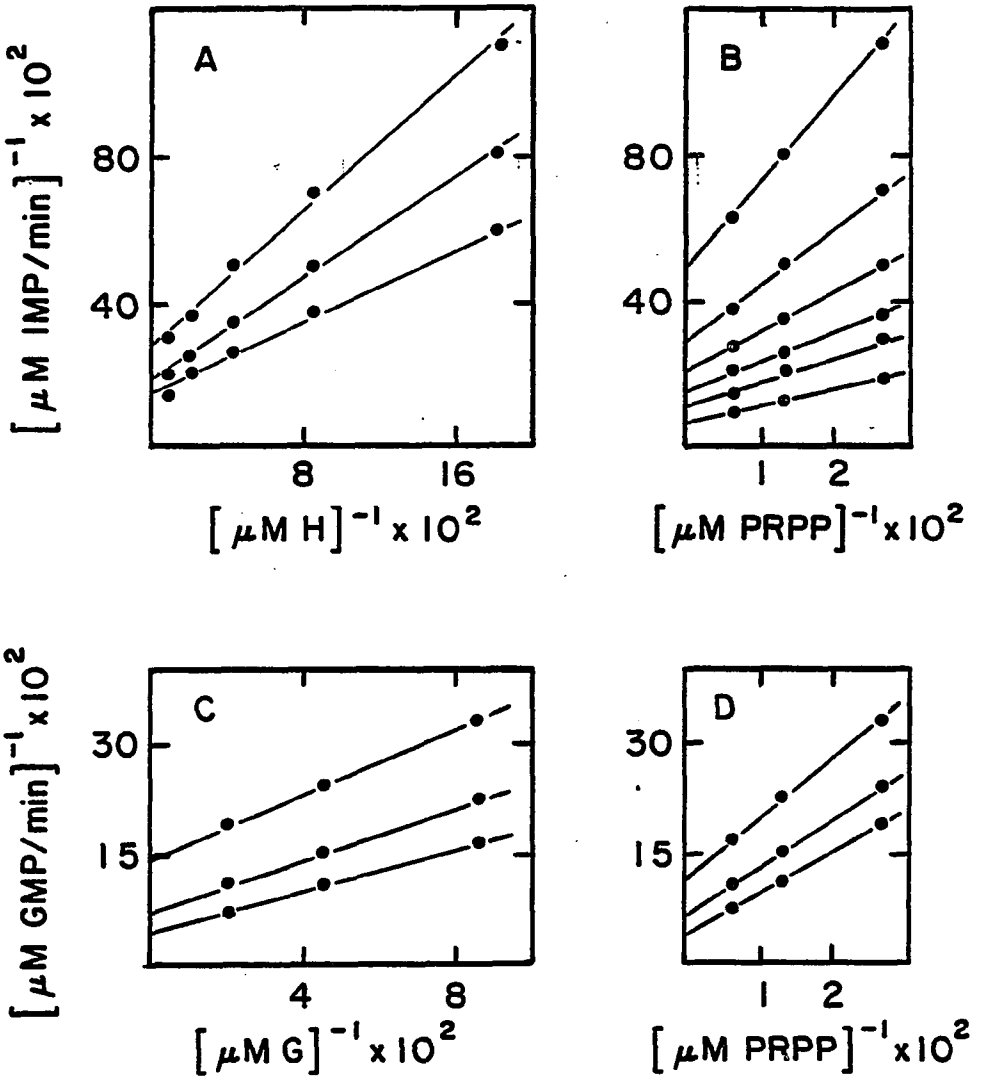
A
B
C
D
80
40
30
15
8
16
4
1
2
[μM IMP/min]⁻¹ x 10²
[μM GMP/min]⁻¹ x 10²
[μM H]⁻¹ x 10²
[μM G]⁻¹ x 10²
[μM PRPP]⁻¹ x 10²
[μM PRPP]⁻¹ x 10²

As shown in Figure 13, where the enzymatic production of IMP was considered, competitive patterns were observed when the reciprocal of the velocity of IMP formation was plotted against the reciprocal of hypoxanthine concentration in the presence of various concentrations of guanine (Figures 13A, 13C, 13E). Three concentrations of PRibPP were employed in the incubation mixture, namely 39 uM (Figure 13A), 77 uM (Figure 13C) and 154 uM (Figure 13E). A secondary plot of the slopes of these three plots (Figure 13G) provided a non-competitive pattern. In contrast, when these reciprocal rates were plotted against the reciprocal of PRibPP concentration (Figures 13B, 13D, 13F) in the presence of various concentrations of guanine, non-competitive patterns emerged. Three concentrations of hypoxanthine were employed, namely, 11.5 uM (Figure 13B), 23 uM (Figure 13D) and 46 uM (Figure 13F). Similarly a secondary plot of the slopes of these three graphs (Figure 13H) provided a non-competitive pattern, the lines of which meet at a point (extrapolated to 24 ± 2 uM guanine) which is analogous to that observed for the above described secondary plot. All of these "One product" data sets do not define a kinetic mechanism for this HG-PRTase catalyzed reaction although the results are consistent with a sequential mechanism during which PRibPP is the first substrate to associate with the enzyme.

Figure 13. Double reciprocal plots of the initial velocity of IMP formation against substrate concentrations in the presence of various fixed concentrations of alternate substrate as determined using the HPLC assay procedure for HG-PRTase. A) Reciprocal rate of IMP formation vs reciprocal hypoxanthine (H) concentration in the presence of 39 uM PRibPP and in the presence of 0 uM G (bottom line), 11.6 uM G (second line), 23.1 uM G (third line) and 46.2 uM G (top line). B) Reciprocal rate of IMP formation vs PRibPP concentration in the presence of 11.6 uM H and in the presence of 0 uM G (bottom line), 11.6 uM G (second line), 23.1 uM G (third line) and 46.2 uM G (top line). C) Same as (A) except that 77 uM PRibPP was employed. D) Same as (B) except that 23.1 uM H was employed. E) Same as (A) except that 154 uM PRibPP was employed. F) Same as (B) except that 46.2 uM H was employed. G) Secondary plots of the slopes of (A), (C) and (E) vs guanine concentration. H) Secondary plots of the slopes of (B), (D) and (F) vs guanine concentration. The lines in this figure were constructed as described in Figure 12.

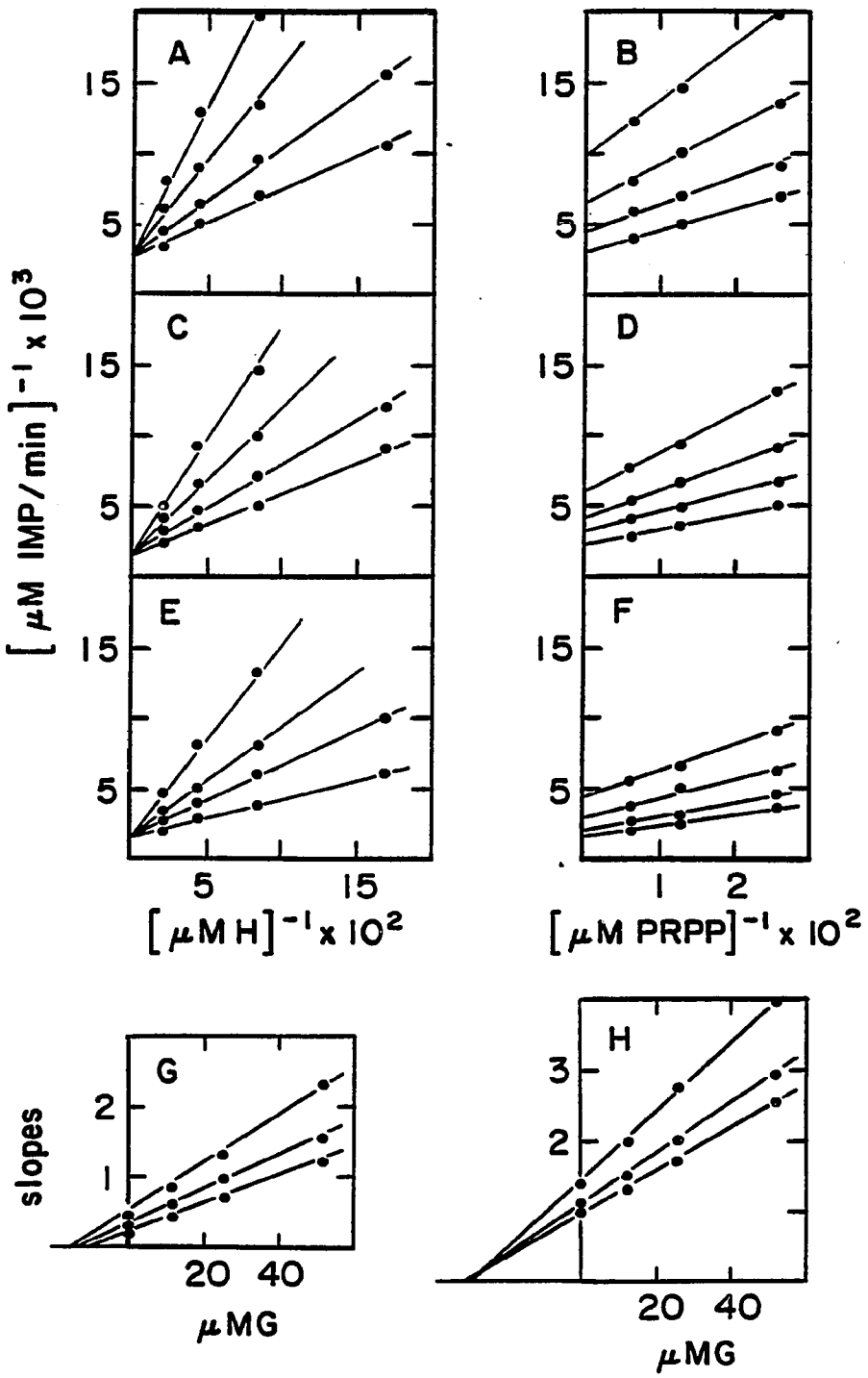
A
B
C
D
E
F
G
H
15
5
1
2
3
20
40
[μM IMP/min]⁻¹ x 10³
[μM H]⁻¹ x 10²
[μM PRPP]⁻¹ x 10²
slopes
μMG
μMG

Results, similar to those calculated for the enzymatic formation of IMP, were observed for the formation of GMP. As shown in Figures 14A, 14C, and 14E, a series of competitive patterns emerged from plots of the reciprocal rates of GMP formation vs guanine concentration in the presence of various concentrations of hypoxanthine and at three different concentrations (39 uM, 77 uM and 154 uM) of PRibPP. In addition, non-competitive patterns were observed when these reciprocal rates were plotted against PRibPP concentration in the presence of various concentrations of hypoxanthine and at three different concentrations (11.5 uM, 23 uM and 46 uM) of guanine (Figures 14B, 14D and 14F). Again secondary plots of the slopes of the data shown in Figures 14A - 14F (Figures 14G and 14H) vs hypoxanthine concentration were non-competitive in nature, in which the lines of both patterns converge at a point which extrapolates to a hypoxanthine concentration value of 62 ± 5 um. These results are consistent with the use of a sequential mechanism by HG-PRTase to form GMP during which PRibPP is the first substrate to bind. Moreover, all of the data illustrated in Figures 12, 13, and 14 can be utilized to characterize the dynamics of the HG-PRTase catalyzed reaction once a specific sequential mechanism can be assigned to these reactions. Analysis of

Figure 14. Double reciprocal plots of the initial velocity of GMP formation against initial substrate concentrations in the presence of various fixed concentrations of alternate substrate as determined using the HPLC assay procedure for HG-PRTase. A) Reciprocal rate of GMP formation vs reciprocal guanine (G) concentration in the presence of 39 uM PRibPP and in the presence of 0 uM H (bottom line), 11.6 uM H (second line), 23.1 uM H (third line) and 46.2 uM H (top line). B) Reciprocal rate of GMP formation vs reciprocal PRibPP concentration in the presence of 11.6 uM guanine and in the presence of 0 uM H (bottom line), 58 uM H (second line), 11.6 uM H (third line), 23.1 uM H (fourth line) and 46.2 uM H (top line). C) The same as (A) except that 77 uM PRibPP was employed. D) The same as (B) except that 23.1 uM guanine was employed and the concentrations of H were 0 uM (bottom line), 11.6 uM (second line), 23.1 uM (third line), 46.2 uM (fourth line) and 92.4 uM (top line). E) The same as (A) except that 154 uM PRibPP was employed. F) The same as (B) except that 46.2 uM guanine was employed and the concentrations of H were 0 uM (bottom line), 11.6 uM (second line), 23.1 uM (third line), 46.2 uM (fourth line), 92.4 uM (fifth line) and 185 uM (top line). G) Secondary plot of the slopes determined in (A), (C), and (E) vs H con-

Figure 14. (cont'd) centration. H) Secondary plot of the slopes determined in (B), (D), and (F) vs H concentration. The lines in this figure were constructed as described in Figure 12.

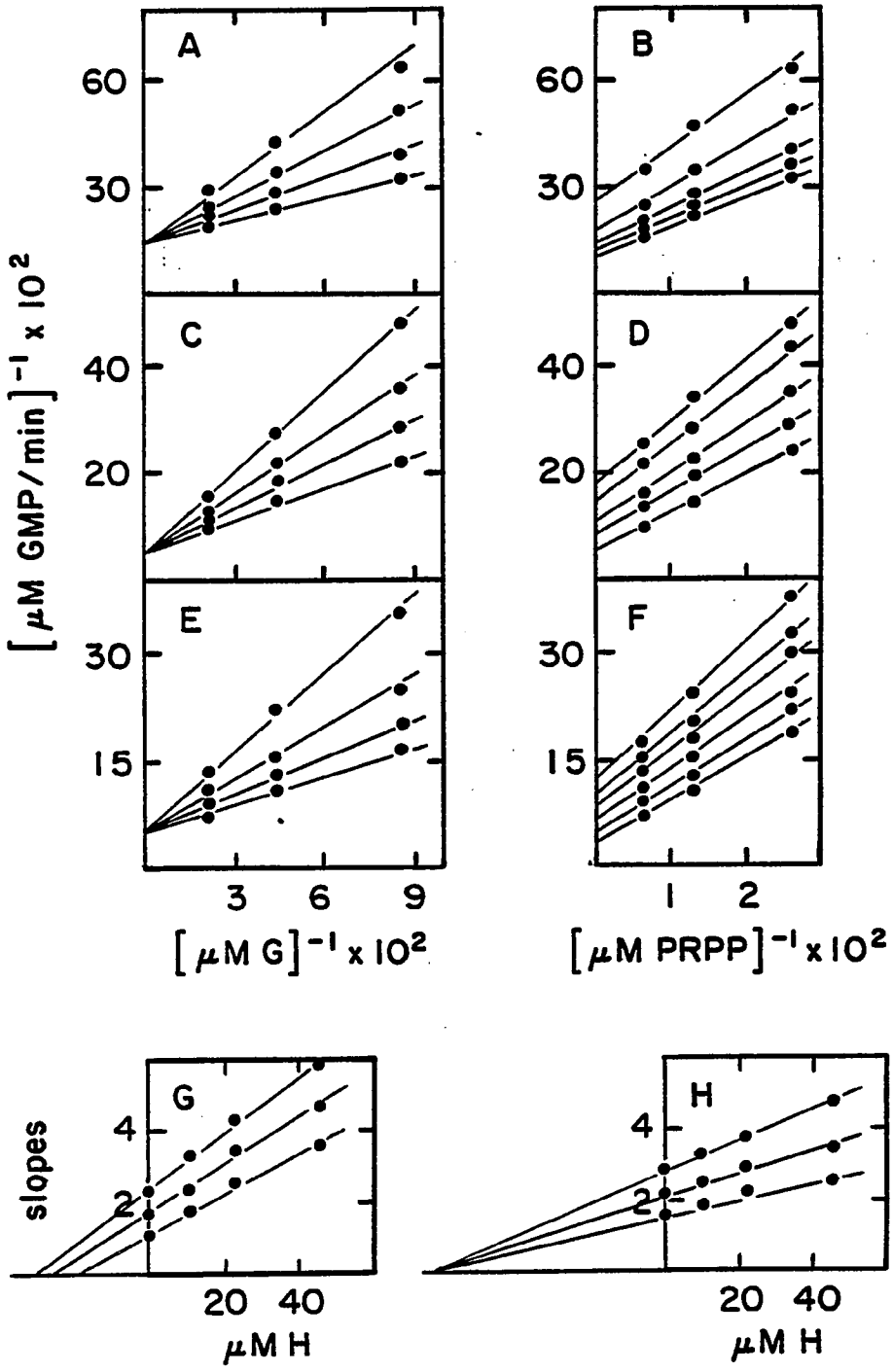
A
B
C
D
E
F
G
H
60
30
40
20
15
4
2
3
6
9
1
2
20
40
[μM GMP/min]⁻¹ x 10²
[μM G]⁻¹ x 10²
[μM PRPP]⁻¹ x 10²
slopes
μM H
μM H

the rates in which a common product (PRibPP utilization which equals PP_i formation) is formed, using the graphical techniques of Huang (79,80), provides a means for such an assignment.

The calculated rates of IMP and GMP formations, under conditions of analogous substrate and alternate - substrate concentrations, were added to arrive at a value for the rate of PRibPP utilization under that set of conditions. Graphical analyses of these compilations are illustrated in Figures 15 and 16. As shown in Figures 15A, 15B and 15C, plots of the reciprocal of the rates of PRibPP utilization multiplied by HG-PRTase concentration (E_o) vs guanine concentrations in the presence of various guanine-to-hypoxanthine initial concentration ratios, are non-competitive in nature with the points of convergences of the lines positioned within the upper right quadrant. These patterns were observed at three different PRibPP concentrations, namely, 154 uM (Figure 15A), 77 uM (Figure 15B) and 39 uM (Figure 15C) and, as described by Huang (79,80), specifically identify guanine as the preferred substrate in the incubation mixture. As shown in Figures 16A, 16B, and 16C, plots of the reciprocal of the rates of PRibPP utilization x E_o vs hypoxanthine concentration, in the presence of various guanine-to-hypoxanthine initial

concentration ratios, are again non-competitive but here the lines of each graph intersect in the left upper quadrant. Similar patterns are observed at the three PRibPP concentrations present in the incubation mixture (39 uM, 77 uM and 154 uM for Figures 16A, 16B and 16C respectively) and these results again suggest that guanine is the preferred substrate of HG-PRTase. If PRibPP is assumed to be the first substrate and either hypoxanthine or guanine to be the second substrate in the sequential kinetic mechanism (proof of this assumption is provided later), then these results elimate the Theorell-Chance mechanism as a possible kinetic mechanism by which HG-PRTase proceeds. Secondary plots of the intercepts shown in Figures 15A-15C and Figures 16A-16C (Figures 15D and 16D respectively) vs PRibPP concentration are observed to be uncompetitive. These patterns are most revealing since, according to theory (79,80) only Ordered BiBi and Ping Pong BiBi mechanisms would be expected to provide such uncompetitive secondary plots. Although the plots of the reciprocal of PRibPP utilization x E_o vs PRibPP concentration, using the constant-ratio alternative substrate method, are not well resolved (Figures 15E-15G and Figures 16E-16J) they all appear to be non-competitive in nature, as are secondary plots of the intercepts of these

graphs (Figures 15H and 16K). According to theory (79,80) the Ping Pong BiBi mechanism can be eliminated as a possible kinetic mechanism with these results. Thus the "common product" data establishes an Ordered BiBi mechanism, during which PRibPP binds to the enzyme first followed by the base substrate, as the sequence by which HG-PRTase catalyzes the formations of IMP and GMP. A summary of this data is given in Table III.

Identification of the kinetic mechanism of the HG-PRTase-catalyzed reactions allowed evaluations of the kinetic constants for both nucleotide formations. The initial velocity results (Figure 12) can be characterized using the following equation (98).

$$\frac{V}{V_{max}} = \frac{[PRibPP][Base]}{K_{i_{PRPP}} K_{m_{Base}} + K_{m_{Base}}[PRibPP] + K_{m_{PRibPP}}[Base] + [PRibPP][Base]} \quad (7)$$

Average calculated values of the Michaels constants (K_m) for PRibPP, hypoxanthine and guanine as well as values for the maximal velocities for IMP and GMP formations (V_H and V_G) and a K_i value for PRibPP are listed in Table IV. Of

Figure 15. Double reciprocal plots of the initial velocity of PRibPP utilization against substrate concentrations in the presence of various fixed G-to-H concentration ratios as determined using the HPLC assay procedure for HG-PRTase. A) Reciprocal rate of PRibPP utilization multiplied by HG-PRTase (E_o) concentration vs the reciprocal of guanine (G) concentration in the presence of 154 uM PRibPP and in the presence of the following G-to-H concentration ratios: ∞ (maximal slope), 2, 1, 0.5 and 0.25 (minimal slope). B) Same as (A) except that 77 uM PRibPP were employed. C) Same as (A) except that 39 uM PRibPP were employed. D) Secondary plot of the y-intercepts of (A), (B) and (C) vs PRibPP concentration. E) Reciprocal rate of PRibPP utilization multiplied by the enzyme concentration vs the reciprocal of PRibPP concentration in the presence of 46.2 uM G and in the presence of the following G-to-H concentration ratios: ∞ (maximal slope, bottom line), 1 and 0.25 (minimal slope, top line). F) Same as (E) except that 23.1 uM G was employed. The following G-to-H concentration ratios were employed: ∞ (maximal slope, bottom line), 1 and 0.25 (minimal slope, top line). G) Same as (E) except that 11.6 uM G was employed. The following G-to-H concentration ratios were employed: ∞ (maximal slope,

Figure 15. (cont'd) top line), 1 and 0.25 (minimal slope, bottom line). H) Secondary plot of the y-intercepts of (E), (F) and (G) vs guanine concentration. Linear least-square analysis was employed to construct the lines of this figure.

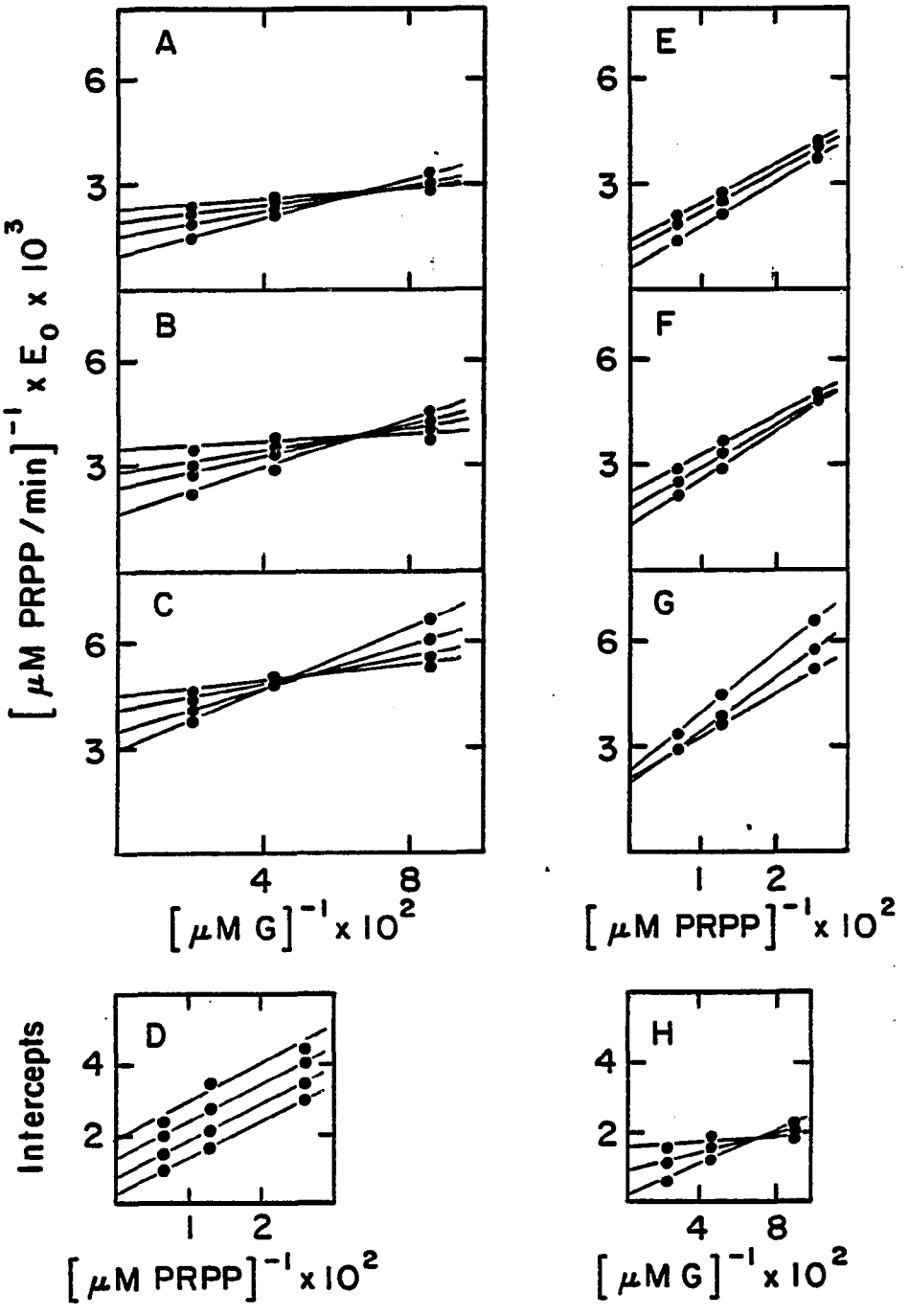
A
B
C
D
E
F
G
H
6
3
4
8
1
2
4
2
$[\mu M\ PRPP/min]^{-1} \times E_o \times 10^3$
$[\mu M\ G]^{-1} \times 10^2$
$[\mu M\ PRPP]^{-1} \times 10^2$
Intercepts

Figure 16. Double reciprocal plots of the initial velocity of PRibPP utilization against substrate concentration in the presence of various fixed G-to-H concentration ratios as determined using the HPLC assay procedure for HG-PRTase. A) Reciprocal rate of PRibPP utilization multiplied by HG-PRTase (E_o) concentration vs hypoxanthine (H) concentration in the presence of 39 uM PRibPP and in the presence of the following G-to-H concentration ratios: 2 (bottom line), 1 (second line), 0.5 (third line) and 0 (top line). B) Same as (A) except that 77 uM PRibPP was employed. C) Same as (A) except that 154 uM PRibPP was employed. D) Secondary plot of the y-intercepts of (A), (B) and (C) vs PRibPP concentration. E) Reciprocal rate of PRibPP utilization multiplied by the enzyme concentration vs the reciprocal of PRibPP concentration in the presence of 92.4 uM H and in the presence of the following G-to-H ratios: 0.5 (bottom line), 0.25 (middle line) and 0 (top line). F) Same as (E) except that 23.1 uM H was employed. The following G-to-H ratios are shown: 2 (bottom line), 1 (second line), 0.5 (third line) and 0 (top line). G) Same as (E) except that 5.8 uM H was employed. The following G-to-H ratios are shown: 2 (bottom line) and 0 (top line). H) Same as (E) except that 184 uM H was employed. The following

Figure 16. (cont'd) G-to-H ratios are shown: 0.25 (bottom line) and 0 (top line). I) Same as (E) except that 46.2 uM H was employed. The following G-to-H ratios are shown: 1 (bottom line), 0.5 (second line), 0.25 (third line) and 0 (top line). J) Same as (E) except that 11.6 uM H was employed. The following G-to-H ratios are shown: 4 (bottom line), 2 (second line), 1 (third line) and 0 (top line). K) Secondary plot of the y-intercepts of (E) through (J) vs hypoxanthine concentration. Linear least-square analysis was employed to construct the lines of this figure.

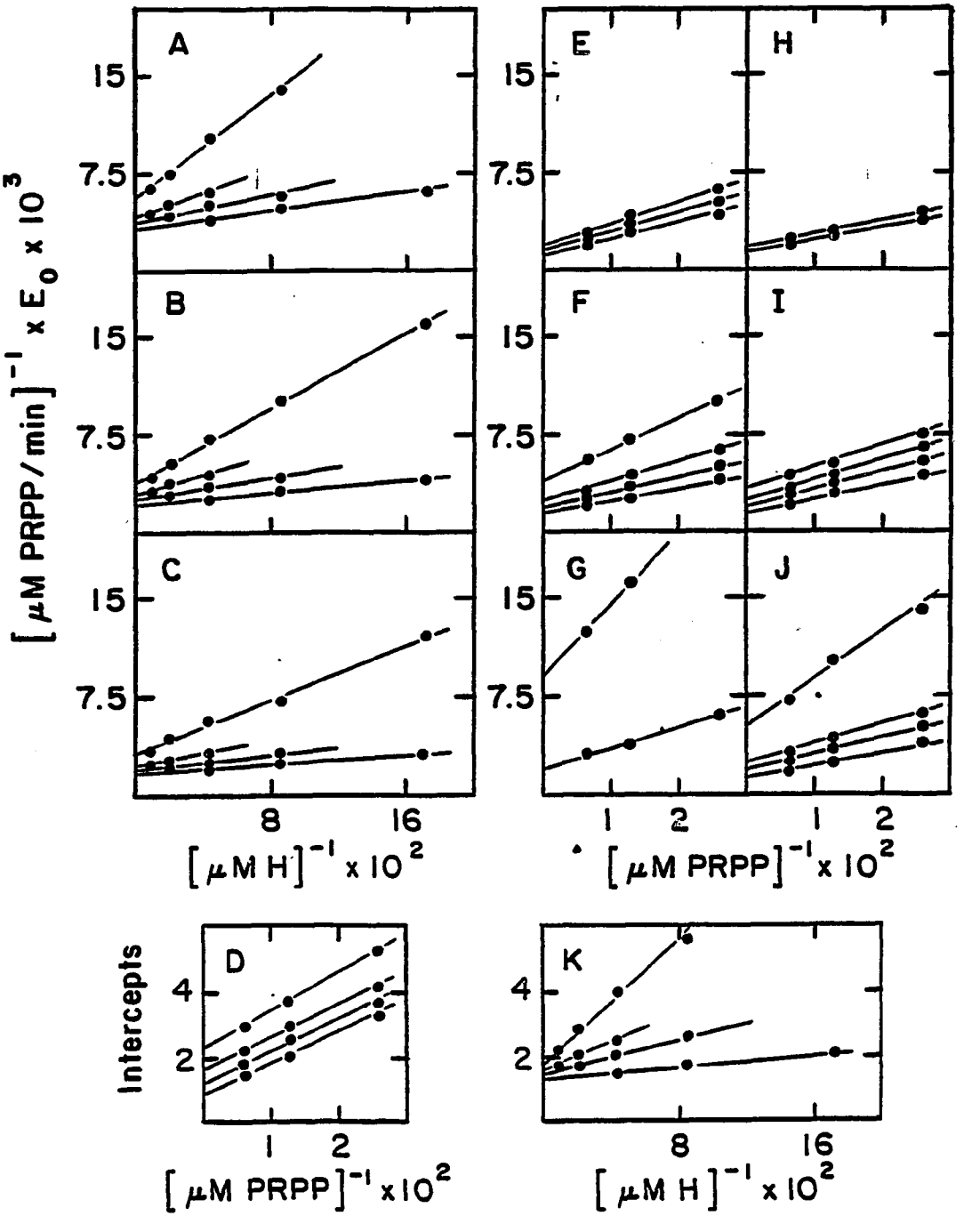
A
B
C
D
E
F
G
H
I
J
K
15
7.5
4
2
8
16
1
2
Intercepts
[μM PRPP/min]⁻¹ x E₀ x 10³
[μM H]⁻¹ x 10²
[μM PRPP]⁻¹ x 10²

TABLE III

A). Predicted Graphical Patterns for the Alternative Substrate Method using the Common-Product Approach.

Mechanism	Alternative Substrate Pair	Varied Substrate			
		A		B	
		1/A Plot	Intercept Plot[a]	1/B Plot	Intercept Plot
Theorell-Chance	BB'	N	C	C	-
Ordered	BB'	N	N	N	U
Rapid Equilibrium Random	BB'	N	N	N	N
Ping-Pong	BB'	U	N	N	U

[a] An intercept plot refers to a plot of the intercepts on the ordinate in a double-reciprocal plot vs the reciprocal of the nonvaried substrate. C, competitive; N, non-competitive; U, uncompetitive.

B). Experimental Results.

Substrate	Alternative Substrate	Varied Substrate					
		PRibPP		Hypoxanthine		Guanine	
		1/PRibPP	Intercept Plot	1/Hypox.	Intercept Plot	1/Gua	Intercept Plot
Hypoxanthine	Guanine	N	N	N	U	-	-
Guanine	Hypoxanthine	N	N	-	-	N	U

TABLE IV

Kinetic Constants for the HG-PRTase-Catalyzed Reaction Determined Using Initial Velocity (IV) and One-Product Alternate-Substrate (OPAS) Procedures

	IMP Formation		GMP Formation	
Parameter[a]	IV	OPAS	IV	OPAS
K_m (PRibPP)	47±5uM		50±5uM	
K_m (H)	26±2uM			
K_m (G)			41±3uM	
K_i (PRibPP)	52±7uM		52±15uM	
K_i (H)		64±5uM		
K_i (G)				23±4uM
V (H)	170±14 units/mg			
V (G)			640±70 units/mg	

[a] Units of activity are defined as nmoles of GMP or IMP formed per min.

interest is the observation that, although guanine has been identified as the preferred substrate, the $Km_{(G)}$ value exceeds slightly that value for hypoxanthine. Thus, for these enzymatic reactions, relative K_m values cannot be used as a criteria for determining substrate perference. However the relative Vmax values do predict a preference by HG-PRTase for guanine and predict that the difference between hypoxanthine and guanine utilization is manifested in the rate-determining step of one or both reactions.

The equations which characterize the initial velocity of an Ordered BiBi Kinetic mechanism in which alternate second substrates are employed are shown below (equations 8 and 9).

$$\frac{V}{V_{max}} = \frac{[PRibPP]}{K_{m_{(PRPP)}}(x_1) + [PRibPP]\ (x_2)} \qquad (8)$$

$$\frac{V}{V_{max}} = \frac{[Base_1]}{K_{m_{(Base_1)}}(x_3) + [Base_1]\ (x_4)} \qquad (9)$$

where:

$$x_1 = 1 + \frac{K_i(PRPP)\,K_m(Base_1)}{K_m(PRPP)\,[Base_1]} + \frac{K_i(PRPP)\,K_m(Base_1)\,[Base_2]}{K_m(PRPP)\,K_i(Base_2)\,[Base_1]}$$

$$x_2 = 1 + \frac{K_m(Base_1)}{[Base_1]} + \frac{K_m(Base_1)\,[Base_2]}{K_m(Base_2)\,[Base_1]}$$

$$x_3 = 1 + \frac{K_i(PRPP)}{[PRibPP]} + \frac{[Base_2]}{K_m(Base_2)} + \frac{K_i(PRPP)\,[Base_2]}{K_i(Base_2)\,[PRibPP]}$$

$$x_4 = 1 + \frac{K_m(PRPP)}{[PRibPP]}$$

Using equations 8 and 9 and the data shown in Figures 13 and 14, average values for K_i (H) and K_i (G) were calculated (Table IV). These values reflect approximately the observed four fold faster rate for enzymatic GMP formation and indicate not only that guanine may bind with a higher affinity to the enzyme than hypoxanthine, but that these binding events may be partially rate limiting.

Flow Dialysis Analysis. A sequence of binding events can be determined directly through the use of an approach to equilibrium dialysis first described by Colowick and

Womack (97). As shown in Figure 17A, the flow of [8-^{14}C]-hypoxanthine through a semi-permeable membrane (10,000 m.w.) is unimpaired and accelerated only slightly by the addition of an 10-fold excess concentration of unlabeled base. Similarly the pattern of diffusion of label through this membrane (Figure 17B) is unimpaired in the presence of 1.4 x 10^{-5} M HG-PRTase and again only slightly affected by successive additions of hypoxanthine. In contrast, (Figure 17C) when both PRibPP and labeled hypoxanthine are added to the upper chamber containing HG-PRTase (1.4 x 10^{-5}M), radioactivity is retained (in the form of hypoxanthine and the product IMP) and its passage through the membrane is accelerated by the addition of increasing concentrations of unlabeled hypoxanthine. Although the binding events illustrated in Figure 17C cannot be characterized because of the presence of two labeled species, the retention of label in this experiment verifies that a hypoxanthine-HG-PRTase interaction can be detected with this procedure. Thus our inability to detect a hypoxanthine-enzyme complex, as shown in Figure 17B, would suggest either that this complex does not form or that the binding affinity of hypoxanthine for HG-PRTase is relatively slight. Moreover, very similar results were obtained when [8-^{14}C]-guanine and the same enzyme

concentration were employed, (Figure 18) suggesting that the guanine HG-PRTase complexation might not occur in solution in the absence of PRibPP.

As shown in Figure 19, the formation of a binary PRibPP-HG-PRTase has been detected and characterized using the flow-dialysis technique. Little if any [1-^{14}C]-PRibPP is observed to flow through the membrane in the presence of 1.4×10^{-5} M HG-PRTase. Successive additions of unlabeled PRibPP to the enzyme solution leads to the appearance of radioactivity in the lower chamber and the addition of a high concentration (2 mM) allows the removal of 95% of the radioactivity from the upper chamber. These results (Figure 19A) and the equations provided by Colowick and Womack (97) were employed to construct a Scatchard plot (Figure 19B). From the intercepts of this plot a K_D value of 2.0±0.2 uM was calculated for the PRibPP interaction with HG-PRTase, and a value of 1.9±0.2 was calculated for n (the number of binding sites). Thus PRibPP binds to two apparently equivalent sites on HG-PRTase with a high affinity. Interestingly the value of K_D is an order of magnitude smaller than the calculated K_m and K_i values of PRibPP as determined by kinetic analysis (Table IV) One explanation for these discrepancies is that a form of

labeled ribose, other than the intact PRibPP molecule, is held by HG-PRTase during the course of the dialysis. Thus we elected to examine HG-PRTase-catalyzed exchange of label between substrate/product pairs.

Isotope Exchange. Victor et.al. (76) employed the exchange of label between [^{32}P]-PPi and PRibPP to establish the labile nature of the ribose-pyrophosphate bond of PRibPP when this substrate interacts with orotate phosphoribosyltransferase (O-PRTase). As shown in Figure 20A, a Dowex-1X8 column can be used to separate PP_i from PRibPP. When HG-PRTase (1.4 uM) is incubated with 1mM Mg^{2+}, [^{32}P]-PP_i and unlabeled PRibPP, 60% of the radioactivity elutes with PRibPP (Figure 20B) suggesting that, like O-PRTase, HG-PRTase catalyzes cleavage of the ribose-pyrophosphate bond in the absence of either base substrate. However, as shown in Figure 20C, the exchange of label was not observed in the absence of Mg^{2+} and the presence of 4 mM EDTA, suggesting that this bond cleavage is dependent upon Mg^{2+}. It would appear, therefore that HG-PRTase may form an enzyme-phosphoribose complex, the production of which may be considered in characterizing PRibPP-enzyme interactions. These results also suggest that HG-PRTase could proceed through the use of a Ping Pong Kinetic mechanism and, in order to examine this

Figure 17. Flow dialysis experiments in which [8-^{14}C]-hypoxanthine is placed in an upper chamber in the presence (B) and absence (A) of 1.4 x 10^{-5}M HG-PRTase, and in the presence of 1.4 x 10^{-5}M HG-PRTase and 100 uM PRibPP (C). The following concentrations of unlabeled hypoxanthine were added to the upper chamber: a) 2 x 10^{-4}M, b) 4 x 10^{-4}M, c) 2 x 10^{-3}M. Experimental conditions: 25°C, 4ml/min flow rate, 10 mM phosphate buffer (pH 7.4) and 1 mM Mg^{2+}.

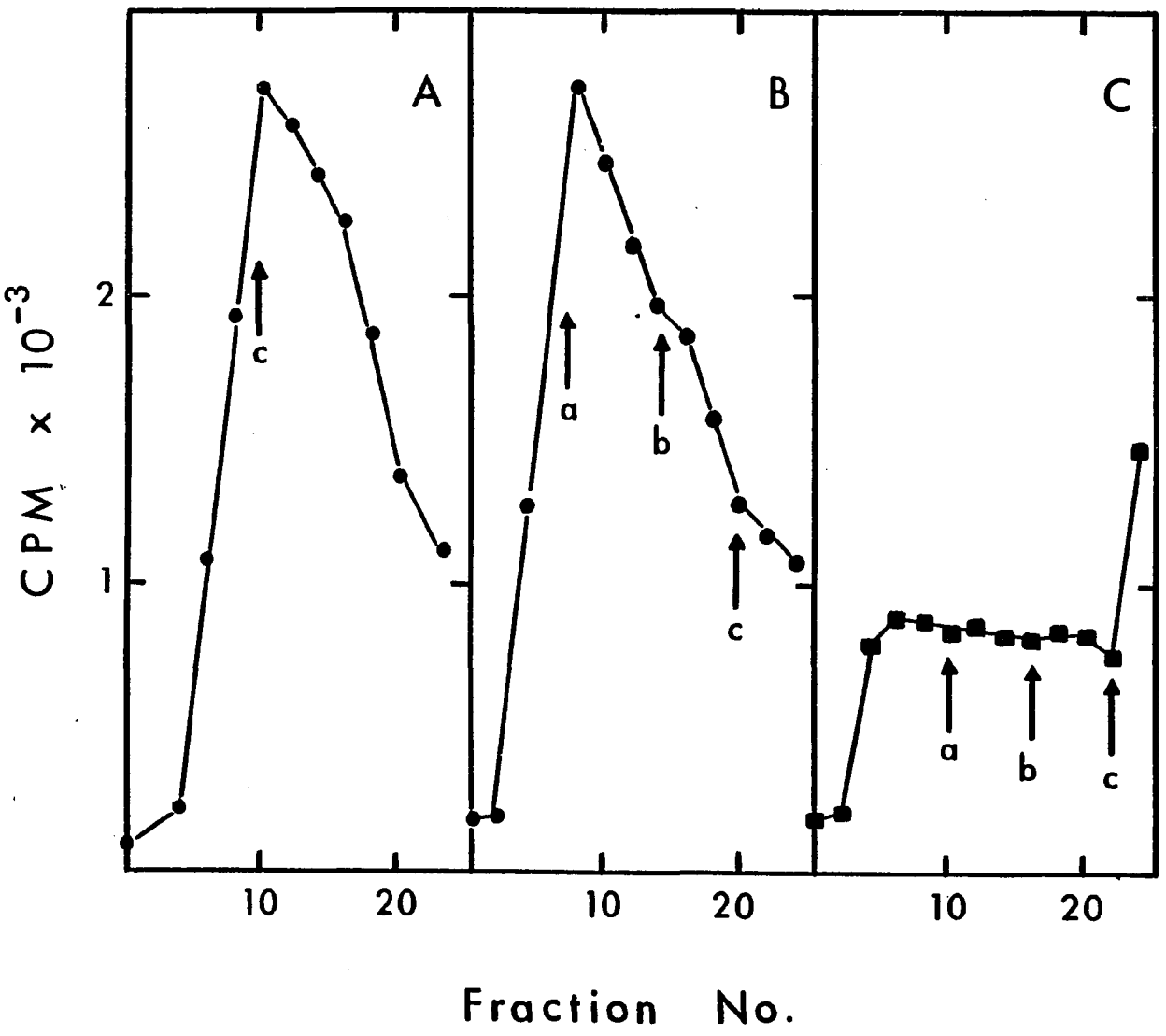
A
B
C
CPM x 10^{-3}
2
1
c
a
b
c
a
b
c
10
20
10
20
10
20
Fraction No.

Figure 18. Flow dialysis experiments in which [8-^{14}C]-guanine is placed in an upper chamber in the presence (B) and absence (A) of 1.4 x 10^{-5}M HG-PRTase, and in the presence of 1.4 x 10^{-5}M HG-PRTase and 100 uM PRibPP (C). The following concentrations of unlabeled guanine were added to the upper chamber: a) 8 x 10^{-5}M, b) 1.4 x 10^{-4}M, c) 1.8 x 10^{-4}M, d) 2.5 x 10^{-4}M and e) 2.5 x 10^{-3}M. Experimental conditions were as described in Figure 17.

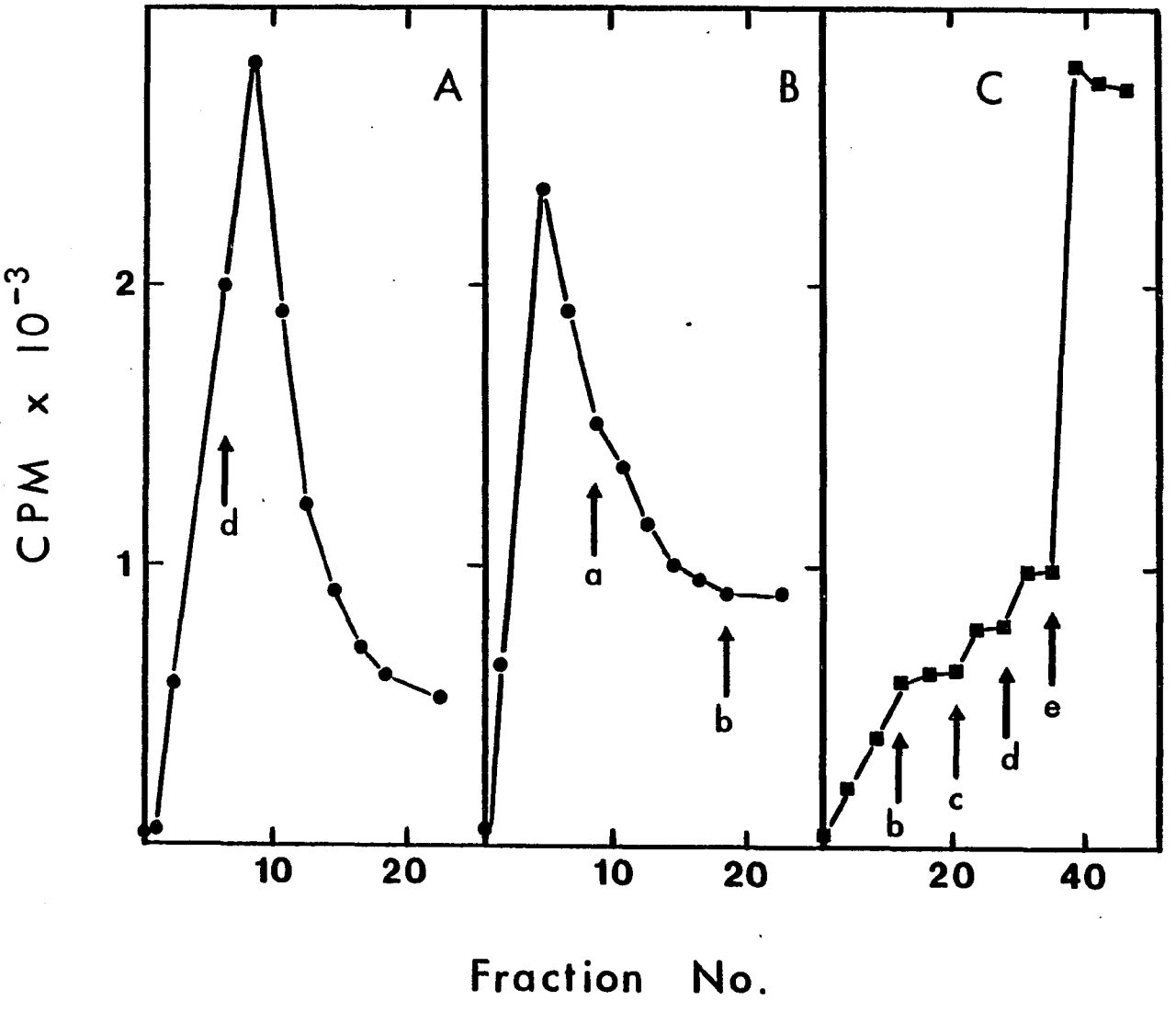
A
B
C
CPM x 10^{-3}
2
1
d
a
b
b
c
d
e
10
20
10
20
20
40
Fraction No.

Figure 19. (A) Flow dialysis experiment in which [1-^{14}C]-PRibPP is placed in an upper chamber with 1.4×10^{-5}M HG-PRTase and (B) Scatchard plot of the data of (A). The following concentrations of unlabeled PRibPP were added to the upper chamber: a) 1.2×10^{-5}M, b) 1.9×10^{-5}M, c) 3.0×10^{-5}M, d) 4×10^{-5}M, e) 2.5×10^{-4}M and f) 2×10^{-3}M. Experimental conditions: 4°C, 4ml/min flow rate, 10 mM phosphate buffer (pH 7.4) and 1 mM Mg^{2+}.

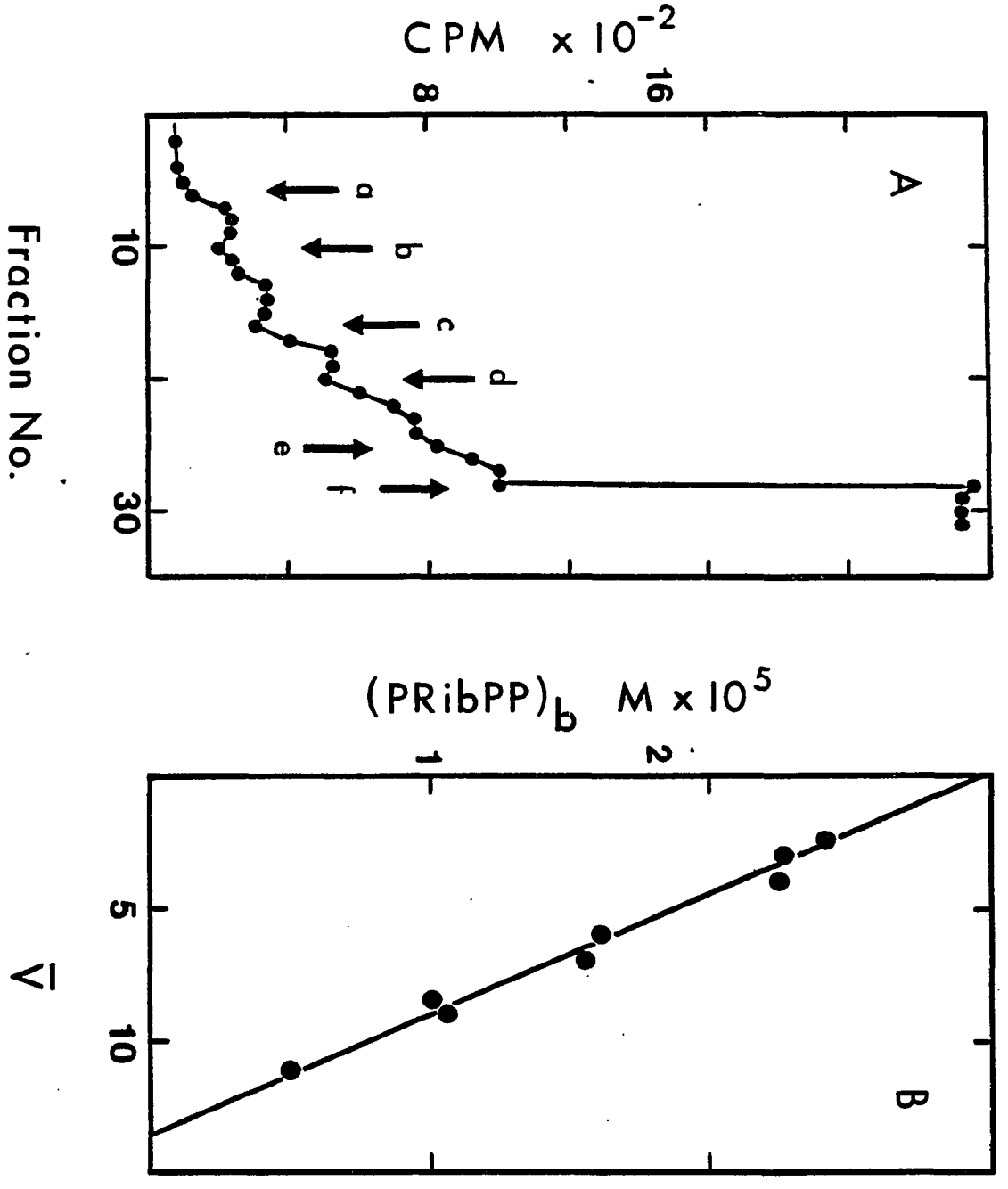
CPM x 10^-2
8
16
A
a
b
c
d
e
f
10
30
Fraction No.
(PRibPP)b M x 10^5
1
2
5
10
V
B

possibility further, we initiated studies of the exchange of labels between [8-^{14}C]-hypoxanthine or [8-^{14}C]-guanine and their respective nucleotides using HPLC separating techniques. As shown in Table V, no exchange of label was observed when HG-PRTase, labeled base and nucleotide were incubated prior to the HPLC injection. Thus unlike yeast O-PRTase but like HG-PRTase from human erthrocytes (16), the HG-PRTase from yeast may not catalyze cleavages of the glycosidic bonds of IMP and GMP.

Figure 20. Dowex 1X8 elution profiles of incubation mixtures composed of: A) [^{32}P]-PP_i and 1 mM PRibPP; B) [^{32}P]-PP_i, 1 mM PRibPP, 1.4 x 10^{-6}M HG-PRTase and 5 mM Mg^{2+}; C) [^{32}P]-PP_i, 1 mM PRibPP, 1.4 x 10^{-6}M HG-PRTase and 4 mM EDTA. Experimental conditions: 4°C, 10 mM phosphate buffer (pH 7.4). Unlabeled PRibPP was detected using the orcinol test (-o-) as described previously by Victor et.al. (76).

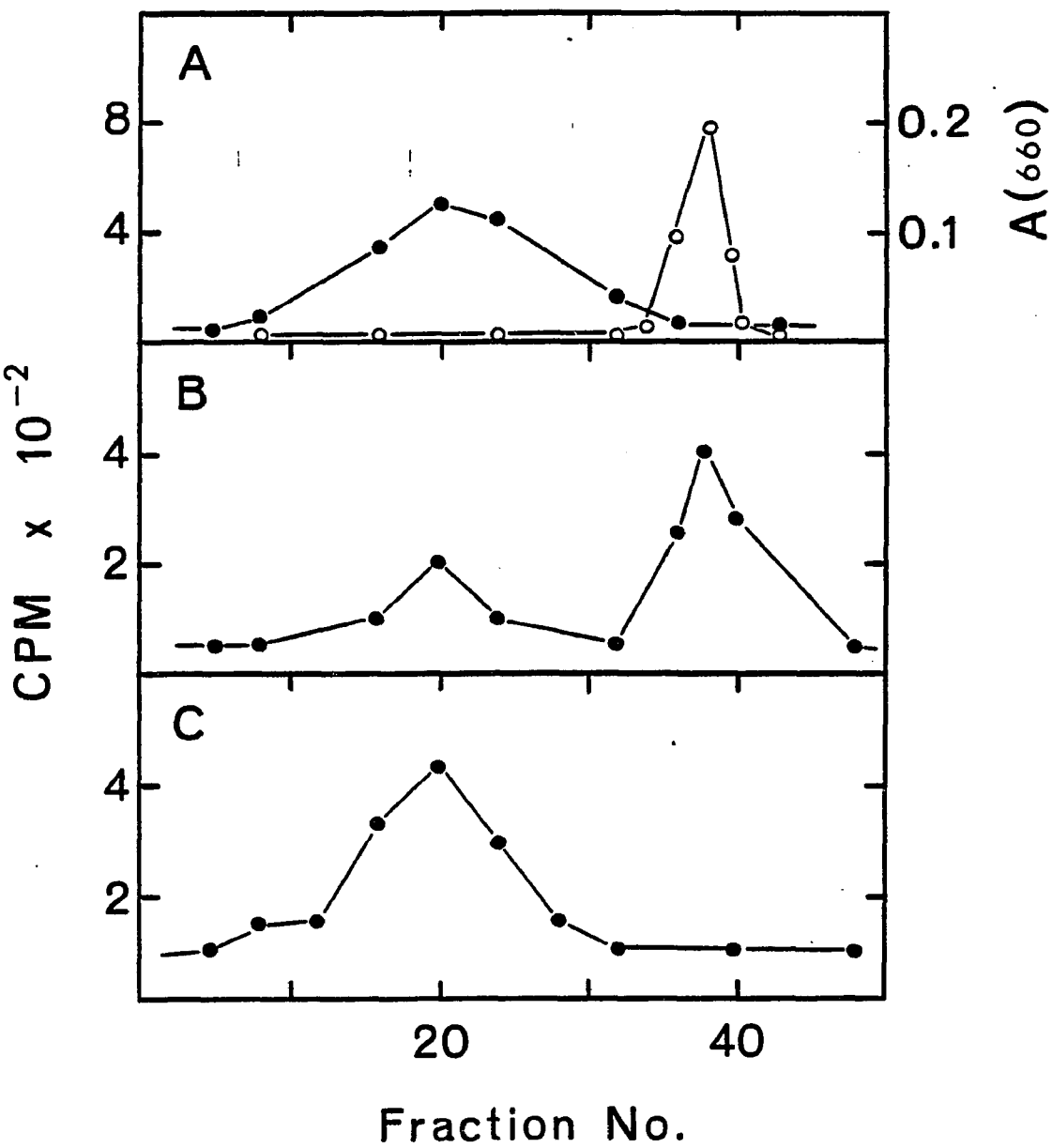
A
B
C
8
4
4
2
4
2
0.2
0.1
A(660)
CPM x 10^{-2}
20
40
Fraction No.

TABLE V

Studies of the HG-PRTase - Catalyzed Exchange of Label Between Substrate/Product Pairs as Determined by HPLC

Incubation Mixture	Radioactivity (CPM)[a]			
	GMP	IMP	G	H
[8-^{14}C]G 167 uM GMP 1.4 uM HG-PRTase	50	-	2048	-
[8-^{14}C]G 167 uM GMP	36	-	1970	-
[8-^{14}C]H 167 uM IMP 1.4 uM HG-PRTase	-	73	-	1990
[8-^{14}C]H 167 uM IMP	-	87	-	1890

a) Locations of the base and nucleotide elutions from the Waters Bondapak C_{18} column were determined using standard 10 ul samples of H, G, IMP and GMP and their 254 nm absorbances.

DISCUSSION

The purification of HG-PRTase was made possible through the use of affinity chromatography which made the isolation procedure more efficient and increased the yield of the purified enzyme from the crude yeast extract.

The native molecular weight of the yeast HG-PRTase determined by gel filtration on Sephadex G-100 was approximately 52,000. Sodium dodecylsulfate gel electrophoresis of the enzyme gave a subunit molecular weight of about 26,000. The values obtained from gel filtration and electrophoresis suggest that the native enzyme consists of two identical or similar subunits. Schmidt et al (11) reported a molecular weight of 51,000 for the native enzyme from Saccharomyces cerevisiae but found no evidence for a subunit structure. Values of 48,000 and 42,000 were reported previously by Nagy and Ribet (10) for the native molecular weight of HG-PRTase from Schizosaccharomyces pombe.

In order to resolve this question about the subunit structure of HG-PRTase from Saccharomyces cerevisiae, covalent cross-linking of the purified enzyme with subsequent analysis of the modified protein on sodium dodecylsulfate gels were employed. Cross-linking of oligomeric

proteins has been employed frequently to determine the subunit structure and the geometrical arrangement of the subunits in the oligomer (81,99,100,101). Davies and Stark (81) have shown that for a protein composed of identical subunits, the number of protein species produced by cross-linking will be equal to the number of subunits in the native protein molecule. The molecular weight of each specie will be equal to integral multiples of the monomer molecular weight. Only two bands corresponding to monomer and dimer were present on sodium dodecylsulfate gels when HG-PRTase was cross-linked with glutaraldehyde. During the shorter incubation period with glutaraldehyde both bands were observed, but after the longer reaction time, the dimer became more predominant. These results suggest that the enzyme most likely exists as a dimer. One explanation for this may be that during the shorter reaction time with glutaraldehyde only a few molecules were cross-linked but as the reaction progressed most of the molecules were cross-linked and were therefore protected from denaturation and reduction upon treatment with sodium dodecylsulfate and β-mercaptoethanol.

Monomeric and dimeric species were observed on SDS gels when the enzyme was cross-linked with dimethyl-suberimidate. The yield of dimers was smaller than that

of monomers. These results may reflect the degree of cross-linking within the molecule, since the monomeric proteins result from a lack of intersubunit cross-linking with dimethylsuberimidate. The mechanism of cross-linking by diimidoesters and glutaraldehyde is similar since the ϵ-amino group of lysyl residues are mainly involved. The reaction with glutaraldehyde leads to the formation of a Schiff base with the amino group whereas dimethylsuberimidate acts by amidination of the amino groups. Cross-linking with glutaraldehyde is facilitated by its size (that is the shorter distance between its two functional groups) and possibly by the greater reactivity in Schiff base formation than amidination reactions. Therefore it can introduce more cross-links per protein molecule than dimethylsuberimidate and this would account for the monomer being the predominant species with dimethylsuberimidate and an increase in dimeric species with glutaraldehyde.

The effect of the substrate, PRibPP, on the cross-linking of HG-PRTase was also investigated, since other researchers have observed that the extent of cross-linking within an oligomeric protein is dependent upon the presence of substrates or inhibitors (101) or allosteric ligands (93). Brew and co-workers (101) have reported that the

substrate, N-acetylglucosamine promoted the cross-linking of the two components of lactose synthetase, L-lactalbumin and a galactosyltransferase with dimethylpimelimidate. Cross-linking studies of the yeast HG-PRTase with glutaraldehyde and dimethylsuberimidate show that the presence of the substrate PRibPP did not influence the extent of intersubunit cross-linking. These results are in agreement with the results reported by Holden and Kelley (9) and Paulus and Bieber (12) for the HG-PRTase from human erythrocytes and beef brain respectively. The results obtained from chemical cross-linking studies suggest that the native enzyme may exist as a dimer and is composed of two identical subunits. Additionally no evidence was found to support the presence of trimeric species or tetrameric species.

Several phosphoribosyltransferases (PRTase) from a variety of sources have been isolated and their kinetic mechanisms have been characterized either partially or completely. Interestingly, both sequential and non-sequential binding events have been defined. For example, bacterial ATP-PRTase (102) proceeds through the use of an Ordered BiBi kinetic mechanism (with ATP serving as the first substrate) whereas orotate-PRTase from yeast (76) makes use of a Ping Pong BiBi mechanism (with PRibPP

serving as the first substrate and with apparent formation of an enzyme-phosphoribosyl intermediate). In contrast Gholson and his collegues (103) have reported that the phosphorylated form of nicotinate-PRTase from yeast may bind PRibPP and nicotinate at random. Of course, characterizations of many PRTase kinetic mechanisms have not been straightforward. Initial-velocity double-reciprocal patterns, consistent with ping pong mechanisms have been observed whereas exchanges of labels between appropriate substrate/product pairs were not detected, suggesting sequential binding events. A study of bacterial anthranilate-PRTase (104) provides such an example. Moreover, adenine-PRTase has been isolated in the form of a covalent enzyme-phosphoribosyl intermediate, perhaps the most straightforward way for concluding that this PRTase proceeds by way of a Ping Pong BiBi kinetic mechanism. Clearly, a single type of kinetic mechanism cannot define how PRibPP is utilized by the PRTase class of enzymes.

Of interest to this discussion, are the previous investigations of the kinetic mechanism of human HG-PRTase. A sequential mechanism was proposed for this enzyme by Henderson et.al. (16), even though initial-velocity double-reciprocal plots were composed of sets of parallel lines, because HG-PRTase-catalyzed exchange of

label between [^{14}C]-guanine and GMP was not observed and because product inhibition analysis argued for an ordered sequence of binding events. Since these results were not consistent with either kinetic mechanism exclusively, these investigators interpreted their initial-velocity plots as being composed of sets of intersecting lines defined by a small value ($<$ 0.1) for the K_i(PRibPP)/K_m(PRibPP) ratio. Krenitsky and Papaioannou (17) re-examined the initial velocity of the human HG-PRTase-catalyzed reactions using a purified preparation of the enzyme and the same assay procedure. These investigators determined that the value of the above-described ratio was in fact greater than 0.1, and they monitored an initial burst of IMP synthesis (a single turnover) upon incubation of hypoxanthine with HG-PRTase, previously incubated with and removed from PRibPP, and with an excess concentration of Mg^{2+}. These results, plus the observation that the initial-velocity double-reciprocal plots were again composed of a series of parallel lines, prompted Krenitsky and Papaioannou to suggest that under conditions of optimal Mg^{2+} concentration (but only under these conditions), PP_i departure from HG-PRTase precedes IMP synthesis. Recently Giacomello and Salerno (8) performed a detailed analysis of both the forward

(phosphoribosyl transfer) and reverse (pyrophosphorolysis) reactions catalyzed by human erythrocyte HG-PRTase using a spectroscopic assay procedure with monitored IMP utilization and synthesis (8), after having characterized the role of Mg^{2+} in these catalyses. Based on their results, Giacomello and Salerno formulated a kinetic model for pyrophosphorolysis in which Mg^{2+} - complexes of IMP and PP_i associate with HG-PRTase in a rapid-equilibrium random fashion whereas hypoxanthine and Mg^{2+} - PRibPP dissociate from the enzyme in that order (8,105). In view of these most recent findings, it would appear that human HG-PRTase proceeds predominantly through the use of a sequential kinetic mechanism. The work of Krenitsky and Papaioannou suggests however that pyrophosphate can dissociate from the ribose portion of PRibPP at the HG-PRTase active site in the absence of either base substrate.

Quite similar conclusions can be drawn from the present studies of the kinetic mechanism of HG-PRTase from yeast. Kinetic analyses using the new HPLC assay procedure and alternate-substrate formulations suggest that an order of binding events occurs during the course of enzyme-catalyzed formations of both IMP and GMP, and the binding studies confirm this conclusion. However, the yeast HG-PRTase also catalyzes an exchange of label

between [^{32}P]-PP_i and PRibPP (but not between labeled base and nucleotide) suggesting that during the course of the phosphoribosyl transfer reaction (but not during pyrophosphorolysis) an HG-PRTase-phosphoribosyl intermediate may form. These results imply that the base substrates could bind to either an enzyme-PRibPP complex or to an enzyme-PRib complex. Nucleotide formation from both associations may result. The base addition to enzyme-PRibPP may accelerate the rate at which PP_i is cleaved from PRibPP relative to that rate in the absence of base, or may accelerate PP_i departure from the active site. In either case, the reaction would appear kinetically to be an SN_2 displacement. Detailed studies of the possible formation of an HG-PRTase-PRib complex are underway currently.

These results demonstrate the use of HPLC procedures to examine PRTase-catalyzed reactions, especially in instances where alternate substrates are known. A great deal of information can be collected in a short amount of time through the use of this type of instrumentation.

REFERENCES

1) Kelley, W.H., and Arnold, W.J., (1973) Fed. Proc. 32, 1656-1659.

2) Olsen, A.S., and Milman, G., (1974) J. Biol. Chem. 249, 4030-4037.

3) Huges, S.H., Wohl, G.M., and Capecchi, M.R., (1975) J. Biol. Chem. 250, 120-126.

4) Hagen, C., (1973) Biochim. Biophys. Acta 292, 105-109.

5) Paulus, V.A., Ingalls, R.G., Vasquez, B., and Bieber, A.L., (1980) J. Biol. Chem. 255, 2377-2382.

6) Hochstadt, J., Meth. Enzymol. (1978) 51, 549-558.

7) Tuttle, J.V., and Krenitsky, T.A., (1980) J. Biol. Chem. 255, 909-916.

8) Giacomello, A., and Salerno, C., (1978) J. Biol. Chem. 253, 6038-6044.

9) Holden, J.A., and Kelley, W.N., J. Biol. Chem. (1978) 253, 4459-4463.

10) Nagy, M., and Ribet, A.M., (1977) Eur. J. Biochem. 77, 77-85.

11) Schmidt, R., Weigand, H., and Reichert, U., (1979) Eur. J. Biochem. 93, 355-361.

12) Paulus, V.A., and Bieber, A.L., (1980) Biochem. Biophys. Res. Comm. 96, 1400-1407.

13) Strauss, M., Behlke, J., and Goerl, M., (1978) Eur. J. Biochem. 90, 89-97.

14) Johnson, G.G., Fisenberg, L.R., and Migeon, B.R., (1979) Science 203, 174-176.

15) Hori, M., and Henderson, J.F., (1966) J. Biol. Chem. 241, 3404-3408.

16) Henderson, J.F., Brox, L.W., Kelley, W.N., Rosenbloom, F.M., and Seegmiller, J.E., (1968) J. Biol. Chem. 243, 2514-2522.

17) Krenitsky, T.A., and Papaioannou, R., (1969) J. Biol. Chem. 244, 1274-1277.

18) Kornberg, A., Lieberman, I., and Simms, E.S., (1955) J. Biol. Chem. 215, 389,402.

19) Fox, I.H., and Kelley, W.N., (1971) Ann. Intern. Med. 74, 424-433.

20) Becker, M.A., Kostel, P.J., and Meyer, L.J., (1975) J. Biol. Chem. 250, 6822-6830.

21) Becker, M.A., Raivio, K.O., Bakay, B., Adams, W.B., and Nyhan, W.L., (1980) J. Clin. Invest. 65, 109-120.

22) Yen, R.C.K., Adams, W.B., Lazar, C., and Becker, M.A., (1978) Proc. Natl. Acad. Sci. U.S.A. 75, 482-485.

23) Atkinson, D.E., and Fall, L., (1967) J. Biol. Chem. 242, 3241-3242.

24) Henderson, J.F. and Khoo, M.K.Y., (1965) J. Biol. Chem. 240, 2349-2357.

25) Fox, I.H., and Kelley, W.N., (1971) J. Biol. Chem. 246, 5739-5748.

26) Hershko, A., Razin, A., and Mager, J., (1969) Biochim. Biophys. Acta. 184, 64-76.

27) Switzer, R.L., and Sogin, D.C., (1973) J. Biol. Chem. 248, 1063-1073.

28) Roth, D.G., Shelton, E., and Deuel, T.F., (1974) J. Biol. Chem. 249, 291-296.

29) Roth, D.G., and Deuel, T.F., (1974) J. Biol. Chem. 249, 297-301.

30) Fox, I.H., and Kelley, W.N., (1972) J. Biol. Chem. 247, 2126-2131.

31) Switzer, R.L., (1971) J. Biol. Chem. 246, 2447-2458.

32) Oslzowy, J., and Switzer, R.L., (1972) J. Bacteriol. 110, 450-451.

33) Hartman, S.C., (1963) J. Biol. Chem. 238, 3036-3047.

34) Kornberg, A., Liberman, I., and Simms, E.S., (1955) J. Biol. Chem. 215, 417-427.

35) Korn, E.D., Remy, C.N., Wasileyko, H.C., (1955) J. Biol. Chem. 217, 875-883.

36) Preiss, J., and Handler, P., (1958) J. Biol. Chem. 233, 493-500.

37) Wegman, J., and DeMoss, J.A., (1965) J. Biol. Chem. 240, 3781-3788.

38) Crowley, G.M., (1964) J. Biol. Chem. 239, 2593-2601.

39) Kelley, W.N., and Wyngaarden, J.B., (1978) The Lesch-Nyhan Syndrome. In The Metabolic Basis of Inherited Disease. J.B. Stanbury, J.B. Wyngaarden, and D.S. Fredrickson, editors. McGraw-Hill Book Co., New York, 4th Edition, Pg 1011-1036.

40) Seegmiller, J.E., Rosenbloom, F.M., and Kelley, W.N., (1967) Science 155, 1682-1684.

41) Boer, P., Lipstein, B., deVries, A., and Sperling, O., (1976) Biochim. Biophys. Acta. 432, 10-17.

42) Beardmore, T.D., Meade, J.C., and Kelley, W.N., (1973) J. Lab. Clin. Med. 81, 43-52.

43) Kennedy, J., (1978) Biochem. Biophys. Res. Commun. 80 653-658.

44) Hershfield, M.S., (1981) J. Clin. Invest. 67, 696-701.

45) Lesch, M., and Nyhan, W.L., (1964) Am. J. Med. 37, 561-570.

46) Kelley, W.N., Rosenbloom, F.M., Anderson, J.F., and Seegmiller, J.E., (1967) Proc. Natl. Acad. Sci. U.S.A. 57, 1735-1739.

47) Nyhan, W.L., (1978) Adv. in Neurology, Vo. 21, Pg 279-287, edited by R.A.P. Kark, R.N. Rosenberg, and L.J. Schut. Raven Press, New York.

48) Nyhan, W.L., (1968) Fed Procc. 27, 1027-1033.

49) Edwards, N.L., Recker, D., and Fox, I.H., (1979) J. Clin. Invest. 63, 922-930.

50) McDonald, J.A., and Kelley, W.N., (1974) Adv. Exp. Med. Biol. 41A, 167-175.

51) Gutensohn, W., and Jahn, H., (1979) Eur. J. Clin. Invest. 9, 43-47.

52) Uitendaal, M.P., de Bruyn, C.H.M.M., Oei, T.L., and Hosli, P., (1978a) Biochem. Genet. 16, 1187-1202.

53) Fox, I.H., and Lacroix, S., (1977) J. Lab. Clin. Med. 90, 25-29.

54) Bakay, B., and Nyhan, W.L., (1975) Arch. Biochem. Biophys. 168, 26-34.

55) Arnold, W.J., and Kelley, W.N., (1971) J. Biol. Chem. 246, 7398-7404.

56) Seegmiller, J.E., (1976) Adv. Hum. Genet. 6, 75-163.

57) Fujimoto, W.Y., and Seegmiller, J.E., (1970) Proc. Natl. Acad. Sci. U.S.A. 65, 577-584.

58) Rijksen, G., Staal, G.E.J., van der Vlist, M.J.M., Beemer, F.A., Troost, J., Gutensohn, W., Van Laarhoven, J.P.R.M., and de Bruyn, C.H.M.M., (1981) Hum. Genet. 57, 39-47.

59) Lyon, M.F., (1961) Nature 190, 372-373.

60) Hellkuhl, B., and Grzeschik, K.H., (1978) Cytogenet. Cell Genet. 22, 527-530.

61) Liskay, R.M., and Evans, R.J., (1980) Proc. Natl. Acad. Sci. U.S.A. 77, 4895-4898.

62) Willecke, K., Klomfass, M., Mierau, R., and Dohmer, J., (1979) Mol. Gen. Genet. 170, 179-185.

63) Graf., L.H. Jr., Urlaub, G., and Chasin, L.A., (1979) Somatic Cell Genet. 5, 1031-1044.

64) Marengo, C., Mbikay, M., Weber, J., and Thirion, J., (1981) J. Virol. 38, 184-190.

65) Kruh, G.D., Fenwick, R.G., and Caskey, C.T., (1981) J. Biol. Chem. 256, 2878-2886.

66) Tong, C., Fazio, M., and Williams, G.M., (1980) Proc. Natl. Acad. Sci. U.S.A. 77, 7377-7379.

67) Foret, M., Schmidt, R., and Reichert, U., (1978) Eur. J. Biochem. 82, 33-43.

68) Housset, P., and Nagy, M., (1977) Eur. J. Biochem. 73, 99-105.

69) Pickering, W.R., and Woods, R.A., (1972) Biochem. Biophys. Acta. 264, 45-58.

70) Polak, A., and Grenson, M., (1973) Eur. J. Biochem. 32, 276-282.

71) Marz, R., Wohlhueter, R.M., and Plagemann, P.G.W., (1979) J. Biol. Chem. 254, 2329-2338.

72) Jackman, L.E., and Hochstadt, J., (1976) J. Bacteriol. 126, 312-326.

73) Roy-Burman, S., and Visser, D.W., (1975) J. Biol. Chem. 250, 9270-9275.

74) Burton, K., (1977) Biochem. J. 168, 195-204.

75) Benson, C.E., Hornick, D.L., and Gots, J.S., (1980) J. Gen. Microbiol. 121, 357-364.

76) Victor, J., Greenberg, L.B., and Sloan, D.L., (1979) J. Biol. Chem. 254, 2647-2655.

77) Vasquez, B., and Bieber, A.L., (1978) Analyt. Biochem. 84, 504-511.

78) Hanna, L., and Sloan, D.L., (1980) Analyt. Biochem. 103, 230-234.

79) Huang, C.V., (1977) Arch. Biochem. Biophys. 184, 488-495.

80) Huang, C.V., (1979) Meth. Enzymol. 63, 486-500.

81) Davies, G.E., and Stark, G.R., (1970) Proc. Natl. Acad. Sci. U.S.A. 66, 651-656.

82) Sinha, S.K., and Brew, K., (1981) J. Biol. Chem. 256, 4193-4204.

83) Chong, P.C.S., and Hodges, R.S., (1981) J. Biol. Chem. 256, 5064-5070.

84) Peters, K., and Richards, F.M., (1977) Annu. Rev. Biochem. 46, 523-552.

85) Rosa, U.Y., and Wold, F., (1977) Adv. Exp. Med. Biol. 86, 169-186.

86) Hoare, D.G., and Koshland, D.E. Jr., (1967) J. Biol. Chem. 242, 2447-2453.

87) Hunter, M.J., and Ludwig, M.L., (1972) Meth. Enzymol. 25, 585-596.

88) Roger, R., and Neilson, D.G., (1961) Chem. Rev. 61, 179-207.

89) Goitein, R.K., Chelsky, D., and Parsons, S.M., (1978) J. Biol. Chem. 253, 2963-2971.

90) Gutensohn, W., Huber, M., and Jahn, H., (1976) Hoppe-Seyler's Z. Physiol. Chem. 250, 120-126.

91) Davis, B.J., (1964) Ann. N.Y. Acad. Sci. 121, 404-427.

92) Wrigley, C.W., (1971) Meth. Enzymol. 22, 559-564.

93) Kapoor, M., and O'Brien, D.O., (1977) Can. J. Biochem. 55, 43-49.

94) Laemli, U.K., (1970) Nature 227, 680-685.

95) Weber, K., and Osborn, M., (1969) J. Biol. Chem. 244, 4406-4412.

96) Flaks, J.G., (1963) Meth. Enzymol. 6, 144-148.

97) Colowick, S.P., and Womack, F.C., (1969) J. Biol. Chem. 244, 774-777.

98) Segal, I.H., (1975) "Enzyme Kinetics", Wiley Interscience, New York.

99) Carpenter, F.H., and Harrington, K.T., (1972) J. Biol. Chem. 247, 5580-5586.

100) Thorner, J.W., and Paulus, H., (1971) J. Biol. Chem. 246, 3885-3894.

101) Brew, K., Shaper, J.H., Olsen, K.W., Trayer, I.P., and Hill, R.L., (1975) J. Biol. Chem. 250, 1434-1444.

102) Morton, D.P., and Parsons, S.M., (1976) Arch. Biochem. Biophys. 175, 677-686.

103) Kosaka, A., Spivey, H.O., and Gholson, R.K., (1977) Arch. Biochem. Biophys. 179, 334-341.

104) Henderson, E.J., Zalkin, H., and Hwang, L.A., (1970) J. Biol. Chem. 245, 1424-1431.

105) Giacomello, A., and Salerno, C., (1979) J. Biol. Chem. 254, 10232-10236.